JAERI-M
89-079

FLUX AND POWER SPECTRA OF PHOTON SOURCES FROM BENDING MAGNETS AND INSERTION DEVICES AT A 8 GEV STORAGE RING

June 1989

Taikan HARAMI

日本原子力研究所
Japan Atomic Energy Research Institute

JAERI-M レポートは，日本原子力研究所が不定期に公刊している研究報告書です。
入手の問合わせは，日本原子力研究所技術情報部情報資料課（〒319-11茨城県那珂郡東海村）あて，お申しこしください。なお，このほかに財団法人原子力弘済会資料センター（〒319-11 茨城県那珂郡東海村日本原子力研究所内）で複写による実費頒布をおこなっております。

JAERI-M reports are issued irregularly.
Inquiries about availability of the reports should be addressed to Information Division Department of Technical Information, Japan Atomic Energy Research Institute, Tokai-mura, Naka-gun, Ibaraki-ken 319-11, Japan.

編集兼発行　日本原子力研究所
印　　刷　いばらき印刷㈱

JAERI-M 89-079

Flux and Power Spectra of Photon Sources from Bending Magnets and Insertion Devices at a 8 GeV Storage Ring

Taikan HARAMI

Synchrotron Radiation Facility Project Team
Japan Atomic Energy Research Institute
Honkomagome, Bunkyo-ku, Tokyo

(Received May 29, 1989)

The synchrotron photon from bending magnets and insertion devices (undulator and wiggler) plays an important role not only for scientific research but also for heat generation on the optical devices in a beam line for a high brilliant synchrotron photon facility. This paper describes the flux and power spectra of the synchrotron photon from bending magnets and insertion devices in a 8 GeV storage ring (electron beam current of 100 mA). The numerical studies show the following results.

(1) The peak power density from a bending magnet is 1.33 kW/mrad^2 in the horizontal plane.
The storage ring having 96 dipoles radiates the total power of 835 kW.

(2) The energy shifter increases the critical energy to 127.7 keV at the magnetic field of 3 tesla.

(3) The multipole wiggler can yield the maximum photon flux of 1.5×10^{15} photons/sec 0.1% band width.
The total radiated power from a wiggler with the peak magnetic field of 1.0 tesla and the length of 4 m is 16.2 kW.
The peak power density is 178 kW/mrad^2 in the forward direction.

(4) The undulator with the length of 2 m and the peak magnetic field of 0.4 tesla yields the total power fo 1.3 kW.
The power density in the forward direction is expected to be between 100 ~ 200 kW/mrad^2, depending on the undulator period and gap.

Keywords: Bending Magnet, Critical Energy, Photon Flux, Power,
Storage Ring, Energy Shifter, Multipole Wiggler,
Power Density, Undulator, Undulator Period and Gap

JAERI－M 89－079

8 GeV蓄積リングにおける偏向電磁石と挿入装置からの光源のフラックスと出力スペクトル

日本原子力研究所大型放射光施設計画チーム
原見　太幹

（ 1989年5月29日受理 ）

高輝度放射光施設における偏向電磁石や挿入装置からの放射光は，光ビームラインの光学機器に熱を発生させることから，そのフラックスと出力を評価しておくことは重要である。この報告は，8GeV蓄積リング（100 mA電流）の偏向電磁石と挿入装置からの放射光のフラックスと出力スペクトルを記述する。解析から次の結果を得た。

(1) 偏向電磁石の出力密度は水平面内で最大1.33 KW／mrad^{2}で，蓄積リング全体（96個分）で835 KWの出力となる。

(2) エネルギーシフタは，3テスラの磁場で臨界エネルギーは127.7 keVである。

(3) 多極ウィグラー（周期数40）からの光フラックス最大は，1.5×10^{15} 光子数／秒・0.1％バンド巾である。

(4) アンジュレータ出力密度は，前方方向で100～200 KW／mrad^{2}程度となり，磁石周期数とギャップに依存する。

日本原子力研究所　：　〒113　東京都文京区本駒込二丁目28－8

Contents

1. Introduction 1
2. Photon sources from bending magnets 2
2.1 Flux 2
2.2 Power spectra 3
3. Photon sources from wiggler 9
3.1 Flux 10
3.2 Power spectra 10
4. Photon sources from undulator 16
4.1 Flux 16
4.2 Power spectra 17
5. Concluding remarks 29
References 30
Appendix 1 Beam emittance and storage ring lattice 31
Appendix 2 Bending magnet in a storage ring 33

目　　次

1. 序 1
2. 偏向電磁石光源 2
2.1 フラックス 2
2.2 出力スペクトル 3
3. ウィグラー光源 9
3.1 フラックス 10
3.2 出力スペクトル 10
4. アンジュレータ光源 16
4.1 フラックス 16
4.2 出力スペクトル 17
5. 結　言 29
参考文献 30
付録1 ビームエミッタンスとストレージリングラティス 31
付録2 ストレージリングの偏向電磁石 33

{NOMENCLATURES}

B_{BM} : bending magnet field,

B_0 : peak magnetic field of undulator,

B_{rig}^{BM} : brightness of photon from bending magnets,

B_{rig}^{WIG} : brightness of photon from wigglers,

c : speed of light ,

e : electron charge,

$E_{p,n}$: photon energy of nth harmonics,

E_b : electron beam energy in storage ring,

E_c : critical energy of photon,

$F_n(K)$: function defined by eq.(26) ,

$F(\gamma\psi)$: function defined by eq.(3) ,

F_{lux}^{BM} : photon flux from bending magnets,

F_{lux}^{WIG} : photon flux from wigglers,

F_{lux}^{UN} : photon flux from undulators,

$f_K(\gamma\theta,\gamma\psi)$: function defined by eq. (32),

G(K) : function defined by eq. (30),

$H(\gamma\psi)$: function defined by eq. (8),

I : electron (or positron) beam current,

K : deflection parameter,

L_{UN} : undulator length,

L_{BM} : length of a bending magnet,

n : harmonic number,

n_e : number density of electron,

N : number of undulator period ,

P : power radiated at all wavelengths,

P_{total}^{BM} : total power radiated from a bending magnet,

P_{total}^{WIG} : total power radiated from a wiggler,

P_{total}^{UN} : total power radiated from an undulator,

$d^2P/d\Omega$: angular distribution of power,

$Q_n(K)$: function defined by eq.(22),

$R(\psi,\theta)$: function defined by eq.(19),

W_s : surface power density defined by eq. (33),

y : direction of undulator magnetic field,

z : direction of electron travelling,

β : electron velocity divided by speed of light,

β_x : betatron function in horizontal direction,

β_y : betatron function in vertical direction,

γ : Lorentz factor, electron energy measured in units of the rest mass of electron,

λ_0 : undulator period ,

λ : photon wavelength,

ε_{CG} : minimum beam emittance in Chassman-Green lattice ,

ζ : function defined by eq. (4),

σ_ψ : rms width of the vertical angle,

ρ : radius of curvature corresponding to the peak field B_0,

ρ_{BM} : bending radius,

θ : polar angle relative to z axis,

Θ : deflection angle of a bending magnet,

ψ : polar angle of electron beam relative to y direction,

1. INTRODUCTION

This preliminary report is intended to present an information on flux and power spectra from bending magnets and insertion devices (undulator and wiggler) at a 8 GeV storage ring. It is expected by using these informations that much closer interaction can be established between users and the accelerator physicists.

The photon from bending magnets and insertion devices can have important application in solid-state spectroscopy, molecular physics, biology and photochemistry. The requirement of various scientific and technological research includes the need for photon with high intensity, specific polarization characteristics, a few micron-sized source, extremely narrow opening angle of photon, tunability of the energy from soft to hard x-rays[1].

We presented the characteristics of undulator sources,i.e. magnet and gap of undulator, tunability from gap variation, brilliance and source size, photon sources for Mössbauer nuclei, in the previous paper[2].

When a very brilliant photon beam is delivered, a large amount of radiated power is also delivered, concentrated in an extremely small solid angle from the low-emittance 8 GeV storage ring. This power need to be handled in a beam line by various elements such as absorbers, masks, filters, pinholes, window and the optical devices (mirrors and monochrometor crystals).

In this report, we describe the characteristics of photon sources from bending magnets and wigglers in chapter 2 and 3, respectively. Flux and power spectra from undulators is discussed in chapter 4. Conluding remarks is given in chapter 5.

2. PHOTON SOURCES FROM BENDING MAGNETS

2.1 Flux

The photon from a bending magnet has a uniform distribution in the horizontal (xz) plane. z is the direction of electron travelling (Fig.1). In the vertical direction y, the brightness (photons/(sec mradθ mradψ 0.1%band width mA)) is a function of angle ψ, and is given by[3]

$$B^{BM}_{trig} = 1.327\times10^{10}E_b^2(\mathrm{GeV})\frac{E_p^2}{E_c^2}F(\gamma\psi), \tag{1}$$

where E_b in GeV is the electron (or positron) energy, E_p in keV is the photon energy and γ is presented by 1957 $\times E_b$. Figure 2 shows the brightness of photon from a bending magnet for the electron beam energy E_b = 8 GeV and the beam current of 100 mA. E_c(keV) is the critical energy and is given by

$$E_c = 0.665E_b^2(\mathrm{GeV})B_{BM}(\mathrm{T}), \tag{2}$$

where B_{BM} is the bending magnet field. Figure 3 gives the critical energy of photon from a bending magnet as functions of the bending field and the electron beam energy. The critical energy is 25.54 keV for B_{BM} = 0.6 tesla and E_b = 8 GeV. $F(\gamma\psi)$ is described by

$$F(\gamma\psi) = (\gamma\psi)^2(1+(\gamma\psi)^2)K^2_{1/3}(\zeta) + (1+(\gamma\psi)^2)^2K^2_{2/3}(\zeta), \tag{3}$$

and

$$\zeta = \left(\frac{E_p}{2E_c}\right)(1+(\gamma\psi)^2)^{3/2}. \tag{4}$$

Figure 4 plotts $(E_p^2/E_c^2)F(\gamma\psi)$ as functions of E_p/E_c and ψ. $K_{1/3}$ and $K_{2/3}$ are Bessel functions of fractional order . Figure 5 shows Bessel functions of $K_{1/3}$ and $K_{2/3}$. For bending magnets, the angular distribution is independent on the horizontal angle θ.

The flux distribution F_{lux} (photons/(sec mradθ 0.1% band width mA)), integrating the brightness over the vertical angle ψ, is given by[3]

$$F^{BM}_{lux} = 2.46\times10^{10}E_b(\mathrm{GeV})\frac{E_p}{E_c}\int_{\frac{E_p}{E_c}}^{\infty}K_{5/3}(y)dy. \tag{5}$$

Figure 6 presents the flux distribution of photon from a bending magnet as a function of E_p/E_c for the 8 GeV electron beam energy and the beam current of 100 mA. Figures 7 and 8 shows the function

$K_{5/3}$ and the integral $G_0(y) = \int_y^\infty K_{5/3}(y)dy$.
The rms width of the vertical angle, σ_ψ, can be approximated as

$$\sigma_\psi = 0.565(E_p/E_c)^{-0.425}\gamma^{-1}. \quad (6)$$

2.2 Power spectra

The power radiated at all wavelengths as a function of angle ψ to the orbit is described by[3]

$$\frac{d^2P}{d\theta d\psi} = 0.0124E_b^4(\mathrm{GeV})B_{BM}(\mathrm{T})H(\gamma\psi) \quad (\mathrm{W/mrad}\theta\,\mathrm{mrad}\psi\,\mathrm{mA}),$$

$$= 0.0413\frac{E_b^5(\mathrm{GeV})}{\rho_{BM}(\mathrm{m})}H(\gamma\psi) \quad (\mathrm{W/mrad}\theta\,\mathrm{mrad}\psi\,\mathrm{mA}). \quad (7)$$

where

$$H(\gamma\psi) = (1+\gamma^2\psi^2)^{-5/2}(7+5(\gamma^2\psi^2)/(1+\gamma^2\psi^2))/16, \quad (8)$$

and ρ_{BM} is the bending radius. Figure 9 shows $H(\gamma\psi)$ as a function of $\gamma\psi$. $H(\gamma\psi = 2) \sim H(\gamma\psi = 0)$ /36.
The power at $\psi = 0$ is given by

$$\frac{d^2P}{d\theta d\psi}(\psi=0) = 5.43\times10^{-3}E_b^4(\mathrm{GeV})B_{BM}(\mathrm{T}) \quad (\mathrm{W/mrad}\theta\,\mathrm{mrad}\psi\,\mathrm{mA}). \quad (9)$$

E_b = 8GeV, B_{BM} = 0.6 T and I = 100 mA yield the power $dP/d\theta d\psi(\psi=0)$ = 1.33 kW/mradθ mradψ radiated in the horizontal plane. We obtain the total radiated power from a bending magnet which is discussed in appendix 2.

$$P_{total}^{BM} = 1.263B_{BM}^2(\mathrm{T})E_b^2(\mathrm{GeV})L(\mathrm{m}) \quad (\mathrm{W/mA}), \quad (10)$$

where L_{BM} is the length of a bending magnet. E_b = 8 GeV, B_{BM} = 0.6 T, L = 3 m and I = 100 mA presents the total radiated power P_{total}^{BM} = 8.7 kW. Symmetric periods, 48, of the storage ring lattice provides the radiation from each bending magnet with the bending angle of 65 mradθ. Thus, the radiation produces the total power integrated over all ψ of 8.7/65 = 133 W per mradθ. It is important to recognize that the power is 133 W/mradθ, whereas the peak power density (ψ = 0) is 1.33 kW/mradθmradψ. The ring having 96 dipoles radiates the total power of 835 kW.

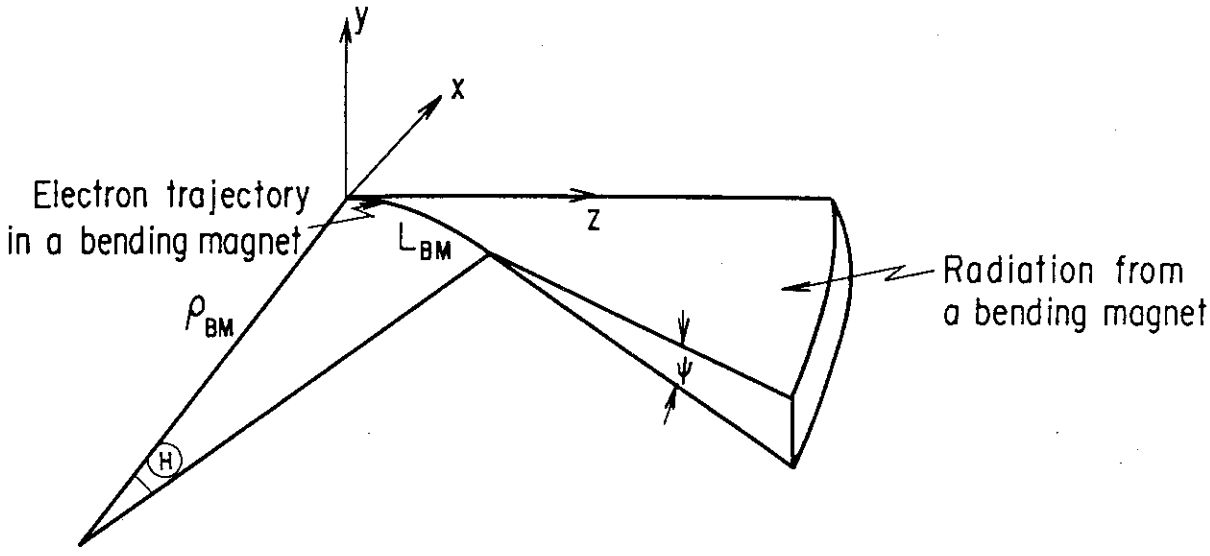

Fig.1 Electron trajectory and coordinate system at a bending magnet.

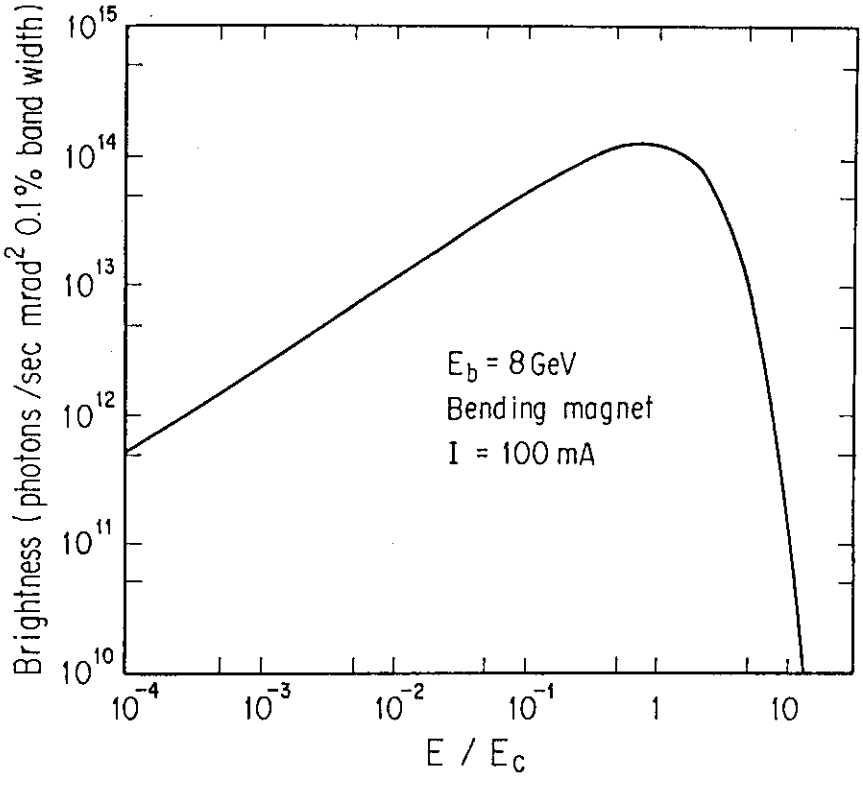

Fig.2 Brightness of photon from a bending magnet with the electron beam energy of 8 GeV and the beam current of 100 mA.

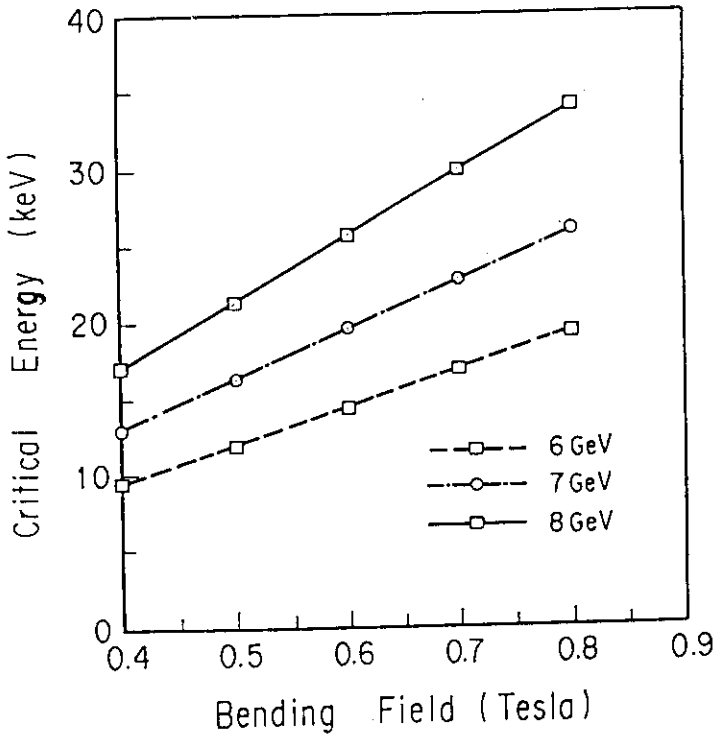

Fig.3 Critical energy of photon from a bending magnet as functions of the bending field and the electron beam energy.

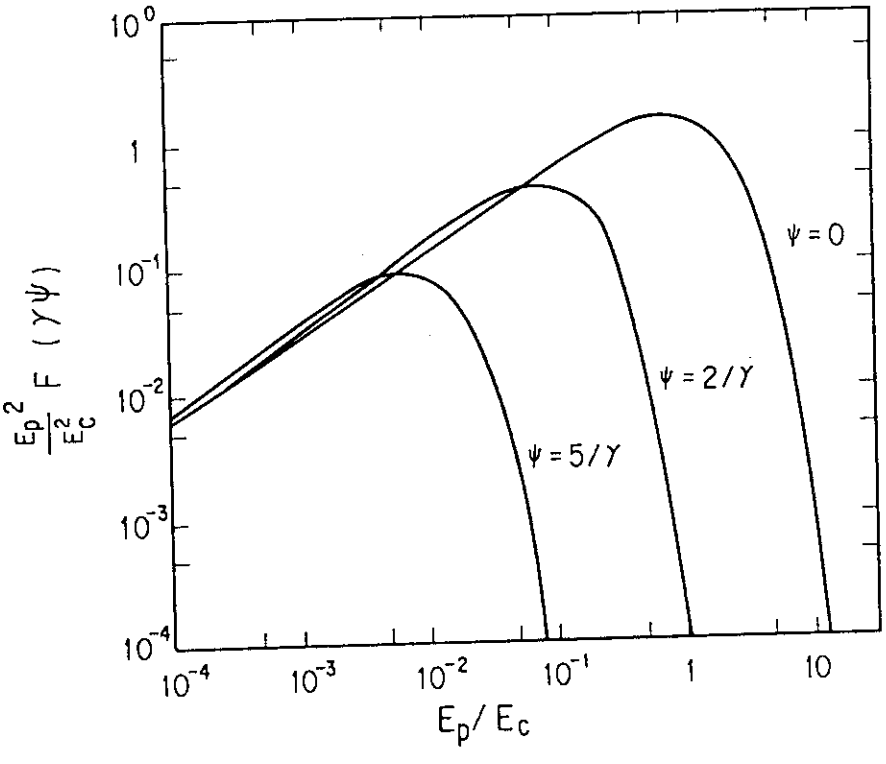

Fig.4 Plotting of the function $(E_p^2/E_c^2)F(\gamma\psi)$ as functions of E_p/E_c and ψ.

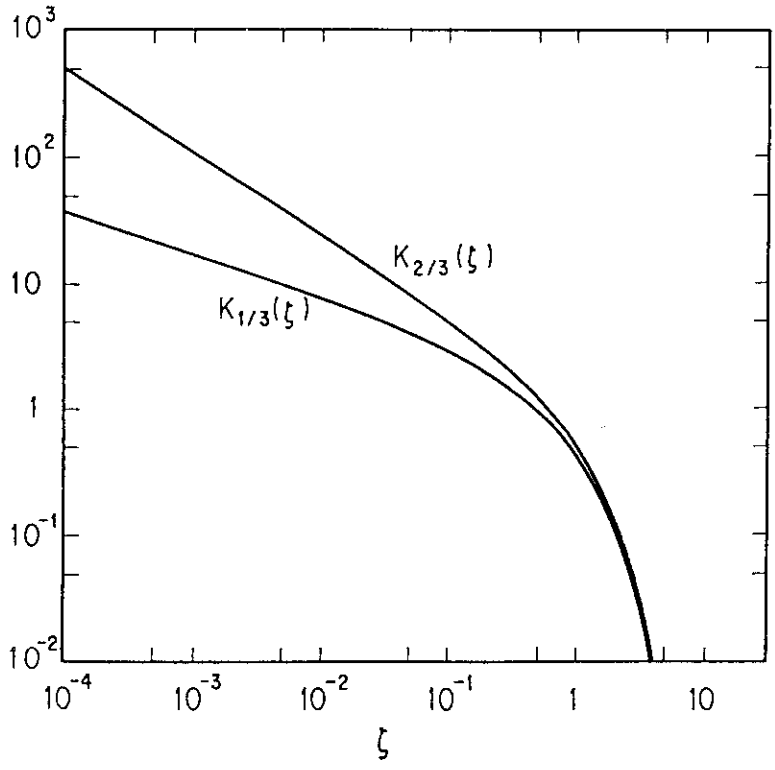

Fig.5 Bessel functions of $K_{1/3}$ and $K_{2/3}$.

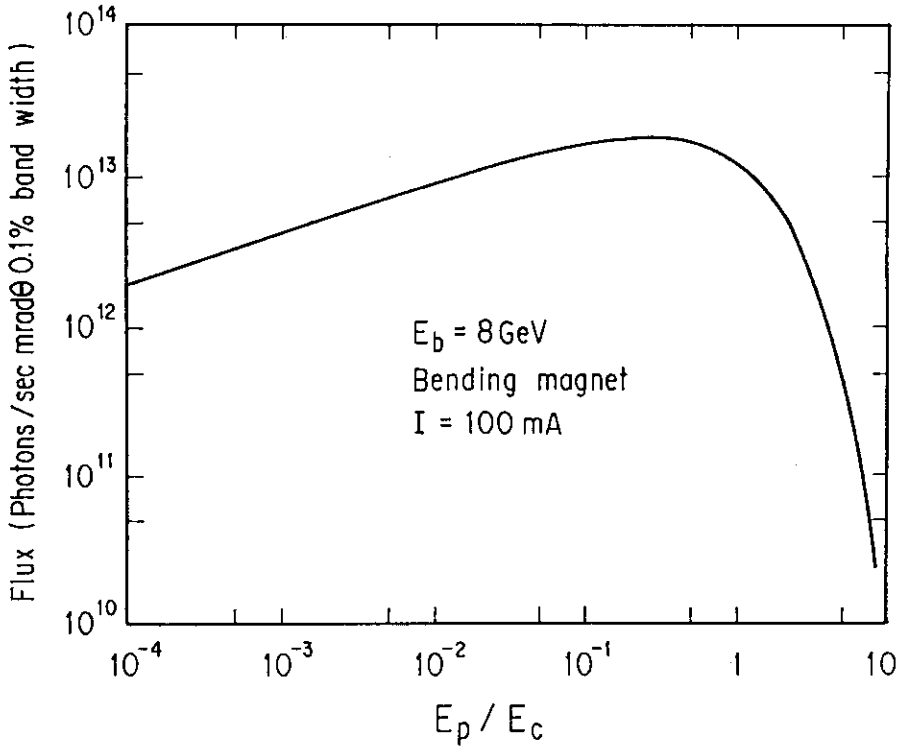

Fig.6 Flux distribution of photon from a bending magnet as a function of E_p/E_c for the electron beam energy of 8 GeV and the beam current of 100 mA.

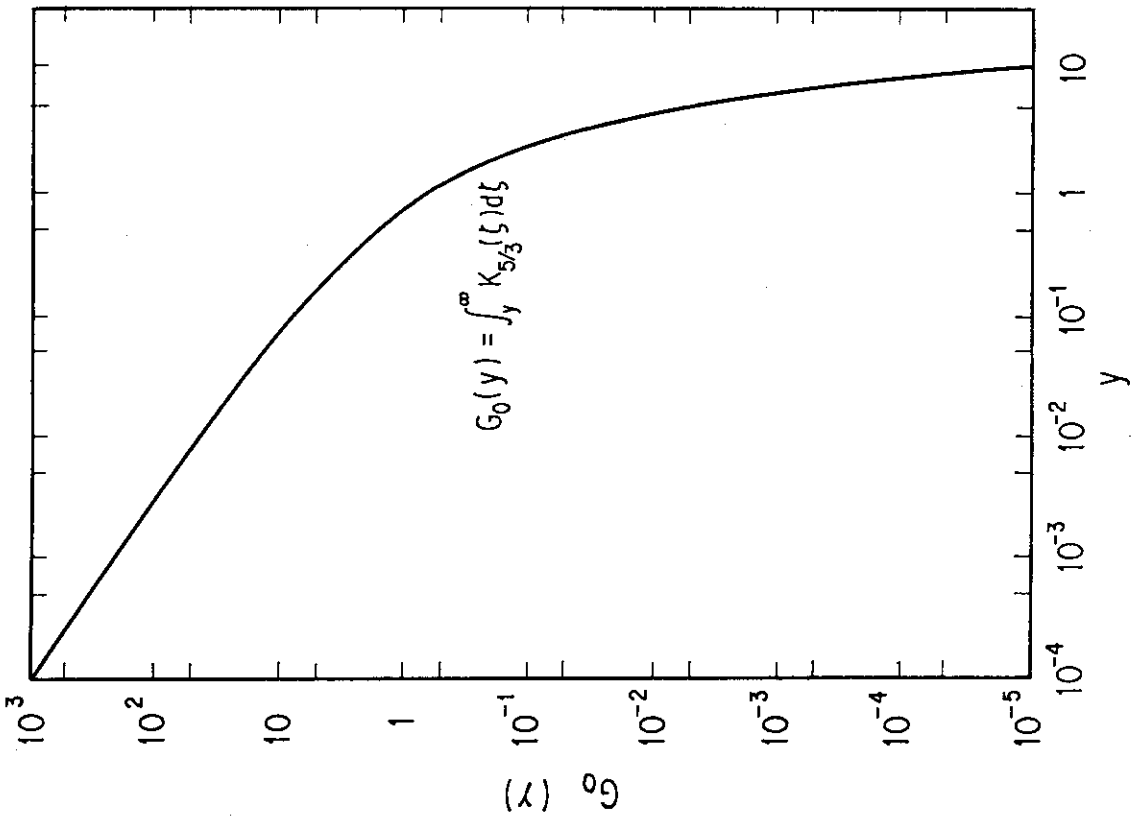

Fig.8 Plotting of the integral $G_0(y)$.

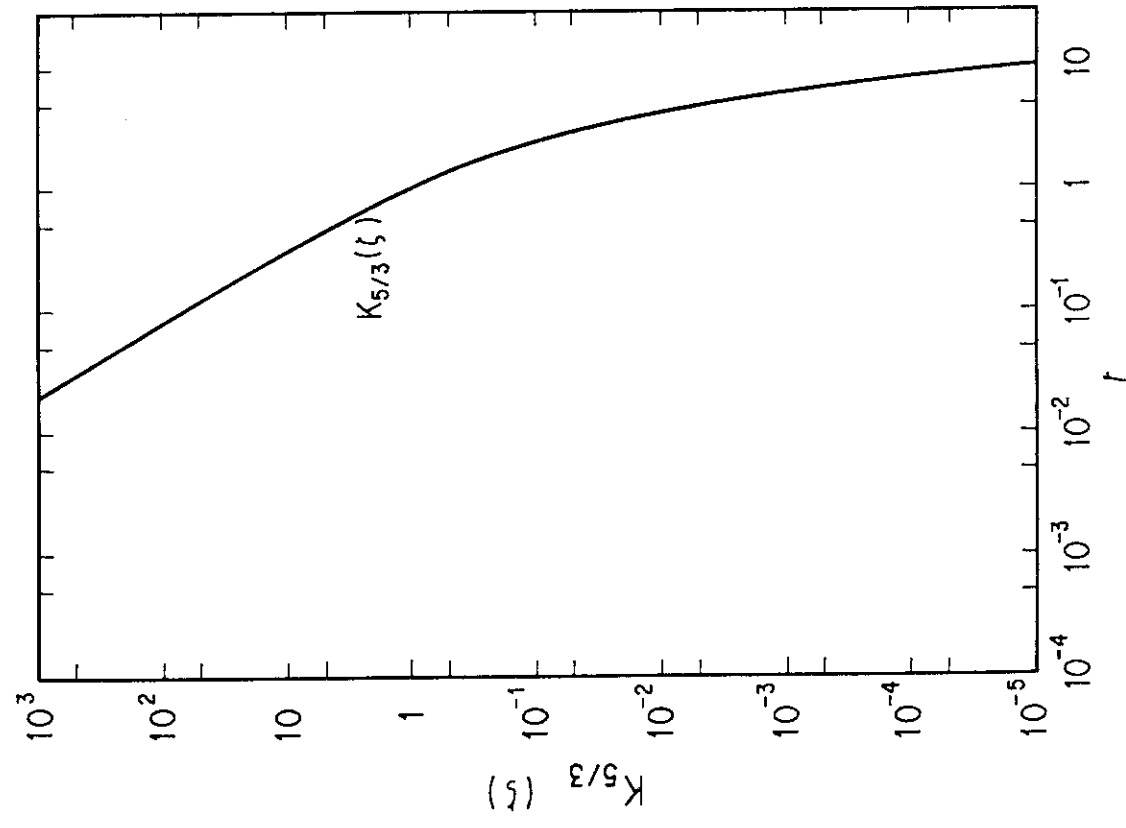

Fig.7 Plotting of the function $K_{5/3}$.

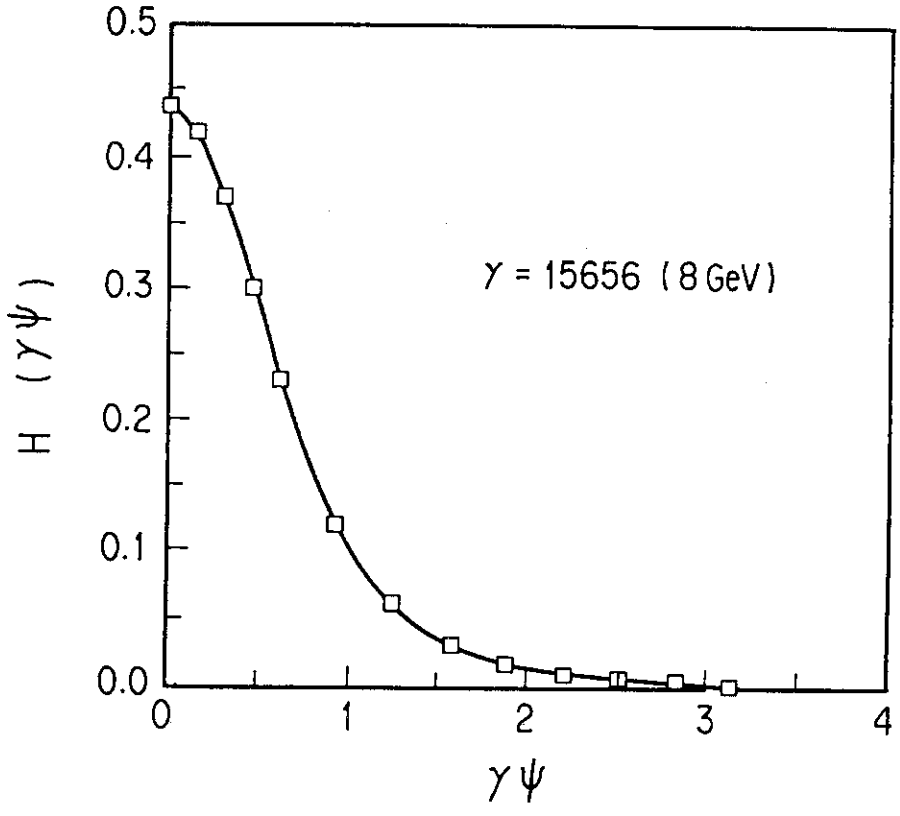

Fig.9 Plotting of the function H($\gamma\psi$) as a function of $\gamma\psi$.

3. PHOTON SOURCES FROM WIGGLER

The critical energy of photon and the flux can be increased by introducing a wiggler in a straight section of a ring[4]. Two types of wigglers can be considered: the energy shifter and the multipole wiggler.

When one wants to increase the photon energy without increasing the total radiated power from a wiggler, this is accomplished by designing a wiggler made up of a single magnetic period with a large magnetic field B_0. Such a wiggler is usually referred to as an "energy-shifter". On the other hand, when one would prefer to have a high flux wiggler with a low value of E_c, this is of special interest for applications where higher photon harmonics are detrimental to the investigation. This so-called "multipole wiggler " can be designed by incorporating multiple periods with low B_0.

The energy shifter increases the critical energy of the radiated spectrum to a value higher than the bending magnet critical energy. For the 8 GeV storage ring, the critical energy is given by

$$E_c(\mathrm{keV}) = 42.56 B_0(\mathrm{T}). \qquad (11)$$

Figure 10 shows the critical energy of photon from a wiggler as a function of magnetic field. B_0 = 3 tesla gives the critical energy of 127.68 keV. The energy shifter usually has 3 poles, with the field of the outer two poles weaker than that of the central magnet. The outer poles act as compensating magnets to match the electron (or positron) trajectory with the ring. The energy shifter is built with either Nd-Fe-B magnets or super conducting magnets, depending on the desired critical energy.

The multipole wiggler on a 8 GeV storage ring is expected to be a low field device (0.5 ~ 1.5 T). These fields can be obtained with the current hybrid magnet technology. The number of periods may vary from 10 to 40, depending on the application and the heat loaded handling capabilities of the optics. Wigglers are distinguished from undulators both by a large value of K and by a high harmonic number n. The spectral peaks of wiggler photon from neighboring smear out because of electron beam emittance effects. The spectral and angular distributions of photon from wigglers become similar to

those of bending magnets, except for a 2N-fold increase of intensity.

3.1 Flux

The brightness of photon for wigglers is multiplied by an additional factor 2N to the equation of a bending magnet.

$$B_{rig}^{WIG}=1.327\times10^{10}E_b^2(\mathrm{GeV})\left(\frac{E_p}{E_c}\right)^2F(\gamma\psi)\times2N. \tag{12}$$

Figure 11 shows the brightness of photon for wigglers with the periods of N = 40, in the horizontal plane of ψ = 0 at E_b = 8 GeV, I = 100 mA. For wigglers, the angular distribution extends to angle $\hat{\delta}$, where $\hat{\delta} = K/\gamma$. Here $\gamma = E_b(\mathrm{GeV}) \times 1957$. The deflection parameter K is given by

$$K = \frac{\gamma\lambda_0}{2\pi\rho} = 0.934B_0\lambda_0, \tag{13}$$

where ρ is the radius of the electron(or positron) trajectory, B_0 is the peak field of undulator in tesla. Integrating the brightness over the vertical angle ψ, the flux distribution F_{lux} is given by

$$F_{lux}^{WIG}=2.46\times10^{10}E_b(\mathrm{GeV})\frac{E_p}{E_c}2N\int_{\frac{E_p}{E_c}}^{\infty}K_{5/3}(y)dy. \tag{14}$$

Figure 12 shows the flux of photon for wigglers with the periods of N = 40 at E_b= 8 GeV and I = 100 mA.

3.2 Power spectra

The photon from a wiggler source has both ψ (yz plane) and θ (xz plane or orbital plane) distributions. The coordinate system is shown in Fig.20 in the following chapter. In designing optics and solving heat load problems, it is essential to evaluate the power densities. The power from a wiggler at θ = 0, integrated for all ψ, is calculated identically to the bending magnet photon. For a wiggler with 2N poles (or N periods)

$$\frac{dP}{d\theta}(\theta=0)=8.45\times10^{-3}E_b^3(\mathrm{GeV})B_0(\mathrm{T})I(\mathrm{mA})N \quad (\mathrm{W/mrad}\theta). \tag{15}$$

Here we used the integral[3],

$$\int H(\gamma\psi)d\psi=\frac{2}{3}\cdot\frac{1}{\gamma}. \tag{16}$$

The total radiated power for a wiggler of length L is given by

$$P_{total}^{WIG}(\mathrm{W})=0.633E_b^2(\mathrm{GeV})B_0^2(\mathrm{T})I(\mathrm{mA})L(\mathrm{m}), \tag{17}$$

or by

$$P^{WIG}_{total}(W) = 7.25\times10^{-3}E_b^2K^2NI/\lambda_0. \quad (18)$$

E_b = 8 GeV, B_0 = 1.0 T, I = 100 mA and L = 4 m yields the total radiated power for a wiggler to be 16.2 kW.

The angular distribution of photon in the horizontal and vertical planes is represented by

$$\frac{d^2P}{d\Omega}(\psi,\theta) = 0.0248E_b^4B_0NIR(\psi,\theta)\ (W/mrad\theta\ mrad\psi), \quad (19)$$

with $R(\psi,\theta) = H(\gamma\psi)\ \cos(\sin^{-1}(\gamma\theta/K))$ [5]. Figure 13 plots $\cos(\sin^{-1}(\gamma\theta/K))$ as a function of θ and K for the 8 GeV electron beam energy. For K = 20, the angular distribution of photon is limited to the angle θ less than 1.28 milliradians in the horizontal plane. The peak power per unit solid angle is

$$\frac{d^2P}{d\Omega}(\psi=0,\theta=0) = 1.085\times10^{-2}B_0(T)E_b^4(GeV)I(mA)N \quad (W/mrad^2). \quad (20)$$

E_b = 8 GeV, B_0 = 1.0 T, I = 100 mA and N = 40 presents the peak power density of 178 kW/mrad^2 in the forward direction.

Figure 14 plots angular power distributions of photon from a multipole wiggler with K = 25.2 and B_0 = 1.5 T.

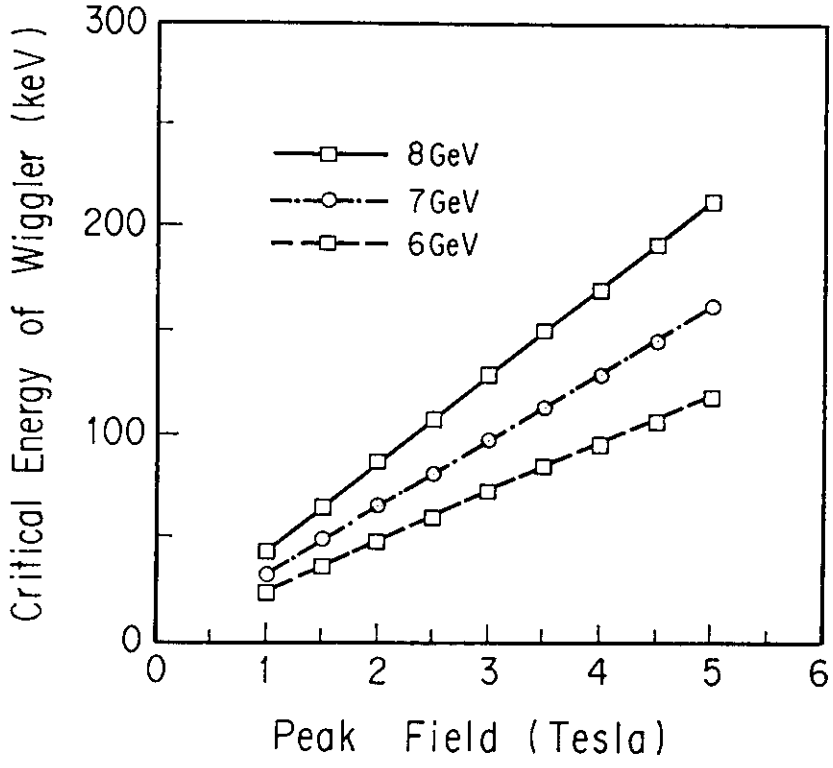

Fig.10 Critical energy of photon from a wiggler as a function of magnetic field.

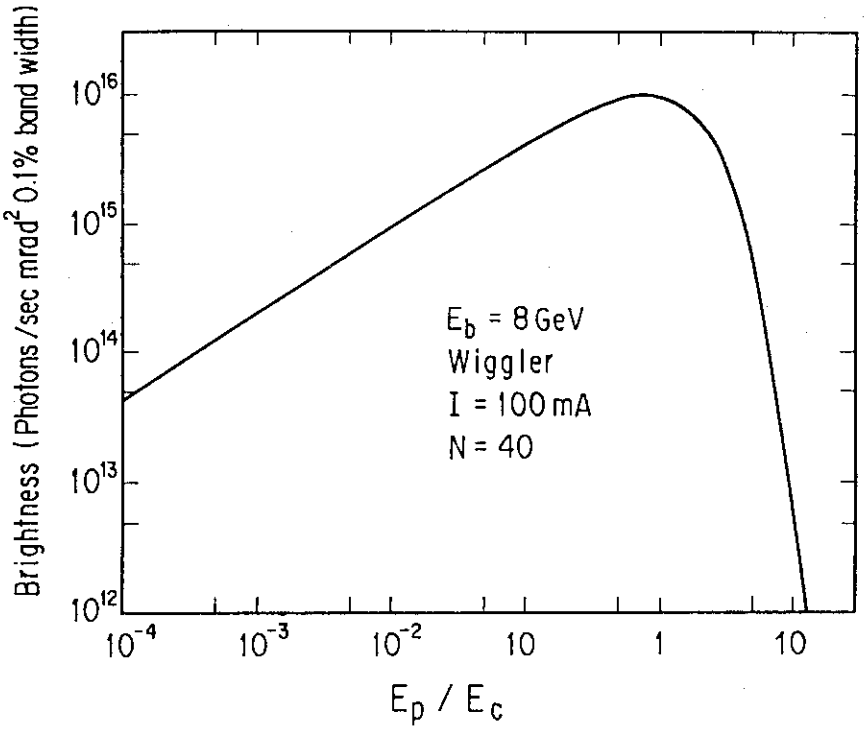

Fig.11 Brightness of photon from a wiggler in the horizontal plane for the electron beam energy of 8 GeV, the beam current of 100 mA and the undulator period of 40.

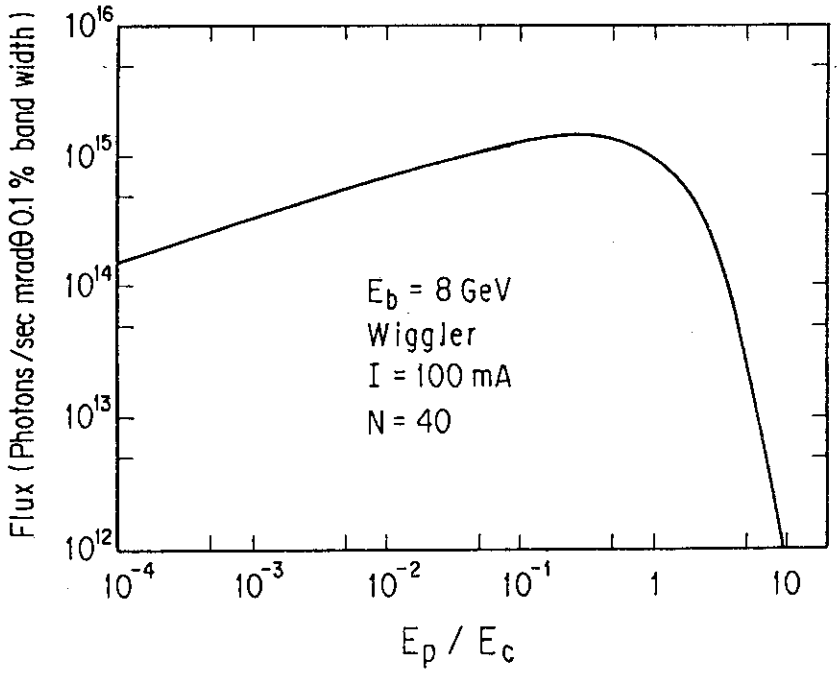

Fig.12 Flux of photon from a wiggler with the periods of 40 for the electron beam current of 8 GeV and the beam current of 100 mA.

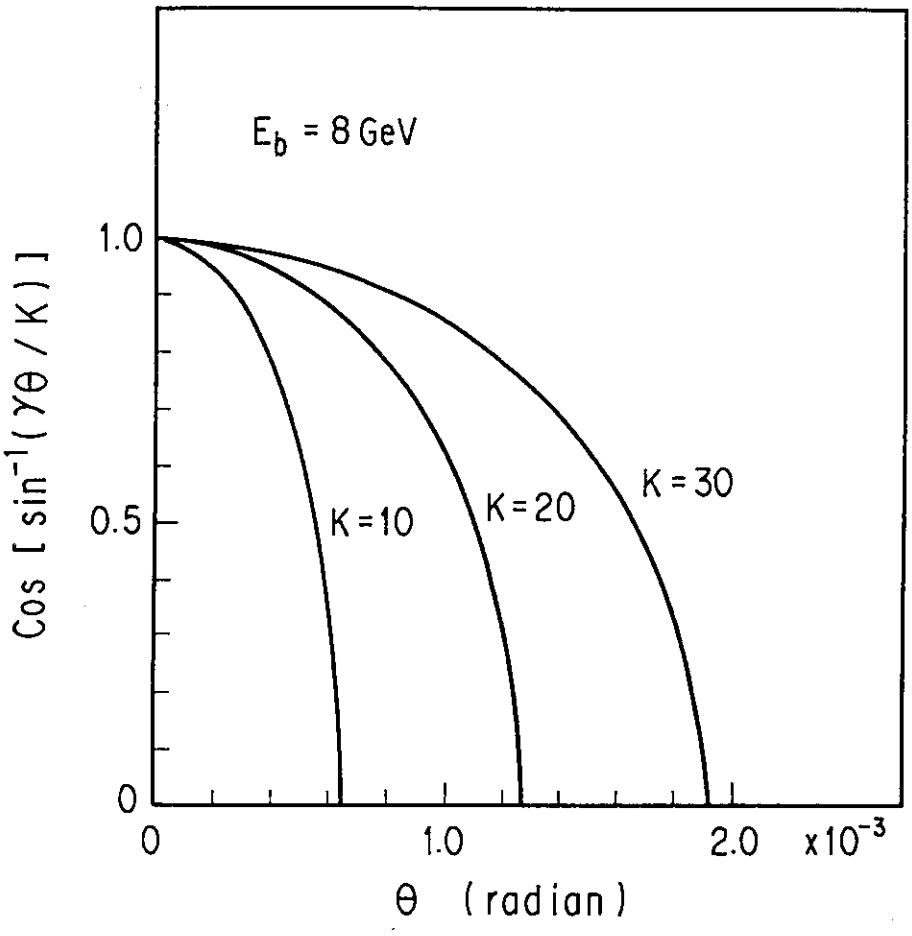

Fig.13 Plotting of the function $\cos(\sin^{-1}(\gamma\psi/K))$ as a function of θ and K.

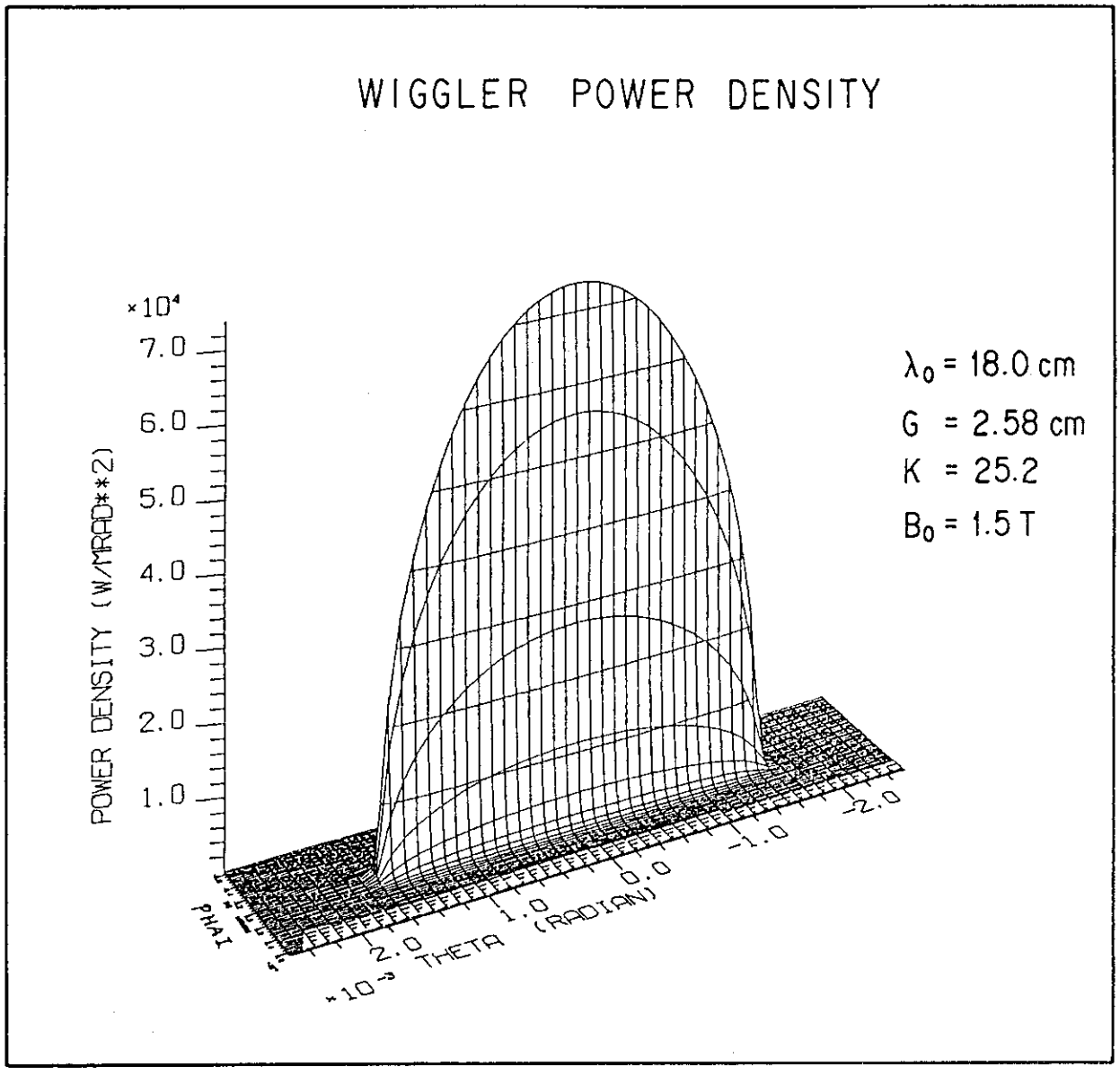

Fig.14 Angular power distributions of photon from a multipole wiggler with K = 25.2 and B_0 = 1.5 T.

4. PHOTON SOURCES FROM UNDULATOR

4.1 Flux

Let us assume the undulator to be L meters long and to have N periods, each λ_0 cm long. With the observer far away from the undulator, the total photon flux (angle integrated) along the undulator axis in the n-th harmonic energy is given by[5]

$$F^{UN}_{lux,n}=1.431\times10^{11}NI(mA)Q_n(K)\left(\frac{\sin N\pi n}{2N\cos\frac{\pi n}{2}}\right)^2, \tag{21}$$

where the function $Q_n(K)$ is given by

$$Q_n(K)=\frac{nK^2}{1+K^2/2}\left(J_{(n+1)/2}(\zeta)-J_{(n-1)/2}(\zeta)\right)^2, \tag{22}$$

and

$$\zeta=\frac{nK^2/4}{1+K^2/2}. \tag{23}$$

Figure 15 shows $Q_n(K)$ as functions of harmonic number, n, and deflection parameter, K.

The unit of $F^{UN}_{lux,n}$ is photons/(sec 0.1% band width). For an undulator with a large number of periods N,

$$F^{UN}_{lux,n}=1.431\times10^{11}NIQ_n(K)=2\pi\sigma_R^2B^{UN}_{rig,0}, \tag{24}$$

where $B^{UN}_{rig,0}$ is described by[6]

$$B^{UN}_{rig,0}=4.555\times10^{4}\gamma^2N^2F_n(K), \tag{25}$$

and $\sigma_R=(\lambda/L)^{1/2}$ (where λ is the photon wavelength and L is the undulator length.). The function $F_n(K)$ is given by

$$F_n(K)=\frac{n^2K^2}{(1+K^2/2)^2}\left(J_{(n-1)/2}(\zeta)-J_{(n+1)/2}(\zeta)\right)^2, \tag{26}$$

where

$$\zeta=\frac{nK^2/4}{(1+K^2/2)}. \tag{27}$$

Figure 16 shows the flux of photon as a function of K at E_b = 8 GeV, I = 100 mA and N = 40. Figure 17 presents the flux of the fundamental harmonic photon as functions of the undulator period, λ_0, and the ratio, G/λ_0, of the undulator gap to period at E_b = 8 GeV, L = 2 m and I = 100 mA. Figures 18 and 19 show the flux of the fundamental and third harmonic photon, respectively, as functions of photon

energy and the undulator period at E_b = 8 GeV, L = 2 m and I = 100 mA. Maximum flux of photon is obtained to be the order of 10^{14} (photons/sec 0.1% band width).

4.2 Power spectra

The angular distribution of the energy integrated power ,$d^2P/d\Omega$, is important in the design of optical elements for high brilliance synchrotron photon sources. For electrons following a sinusoidal trajectory, $d^2P/d\Omega$ is expressed in a general formula[7]

$$\frac{d^2P}{d\Omega}(W/rad^2)=\frac{d^2P}{d\theta d\psi}=P_{total}^{UN}\frac{21\gamma^2}{16\pi K}G(K)f_K(\gamma\theta,\gamma\psi), \tag{28}$$

where P_{total}^{UN} is the total power (integrated over angles and energy) given by

$$P_{total}^{UN}(W)=0.633E_b^2(GeV)B_0^2(T)L(m)I(mA). \tag{29}$$

Figure 20 shows the electron trajectory and coordinate system. The electron moves on a sinusoidal trajectory in the horizontal plane x-z. θ and ψ are the angles of observation in the horizontal and vertical directions, respectively. E_b = 8 GeV, B_0 = 0.4 T, L = 2 m and I = 100 mA yields the total power P_{total} = 1.3 kW. Figure 21 shows the total power of photon as functions of the fundamental harmonic photon energy and the undulator period at E_b = 8 GeV, L = 2 m and I = 100 mA. The total power increases with large λ_0.

G(K) is a normalization factor given by

$$G(K)=K\frac{K^6+\frac{24}{7}K^4+4K^2+\frac{16}{7}}{(1+K^2)^{7/2}}. \tag{30}$$

Figure 22 shows G(K) as a function of deflection parameter K.

$f_K(\gamma\theta,\gamma\psi)$ is a factor which gives the angular dependence as follows:

$$f_K(\gamma\theta,\gamma\psi)=\frac{16K}{7\pi G(K)}\int_{-\pi}^{\pi}d\alpha\left(\frac{1}{D^3}-\frac{4(\gamma\theta-K\cos\alpha)^2}{D^5}\right)\sin^2\alpha, \tag{31}$$

where $D = 1 + (\gamma\psi)^2 + (\gamma\theta - K\cos\alpha)^2$. Figure 23 shows the function U in the integral of eq. (31) at θ = 0 and ψ = 0.

$$U=\left(\frac{1}{D^3}-\frac{4(K\cos\alpha)^2}{D^5}\right)\sin^2\alpha, \tag{32}$$

The function U has the nonzero value near $\alpha = -\pi/2$ and $\pi/2$. The function f_K is normalized so that $f_K(0,0) = 1$.

Figures 24 through 26 show the function $f_K(\gamma\theta,0)$ as functions of

K, θ and $\gamma\theta$. $f_K(\gamma\theta,0)$ extends over the region of angle $\theta = K/\gamma$. Figures 27 and 28 show the function $f_K(0,\gamma\psi)$ as functions of K, ψ and the electron beam energy E_b. $f_K(0,\gamma\psi)$ does not depend greatly on the value of K, but on the electron beam energy. The power density in the forward direction is

$$\frac{dP}{d\Omega}(0,0) = 10.84 B_0(T) E^4(GeV) I(A) NG(K) \quad (W/mrad^2). \tag{33}$$

Figure 29 presents the power density of photon in the forward direction as functions of the fundamental harmonic photon energy and undulator period at E_b = 8 GeV, L = 2 m and I = 100 mA. The power density in the forward direction is expected to be between 100 ~ 200 kW/mrad^2, depending on the undulator period and gap.

Figures 30 and 31 plot the angular power distributions of photon from undulators, varying K as a parameter. As K increases, photon diverses to wide range of angle θ.

It is often useful to consider the power distribution on a surface located S meters away from the center of the ID(insertion device). The normal radiation impinging on a surface can be defined by peak surface power density W_s (in W/mm^2) which is given by

$$W_s = \frac{d^2P}{d\theta d\psi}(\theta=0,\psi=0)/S^2. \tag{34}$$

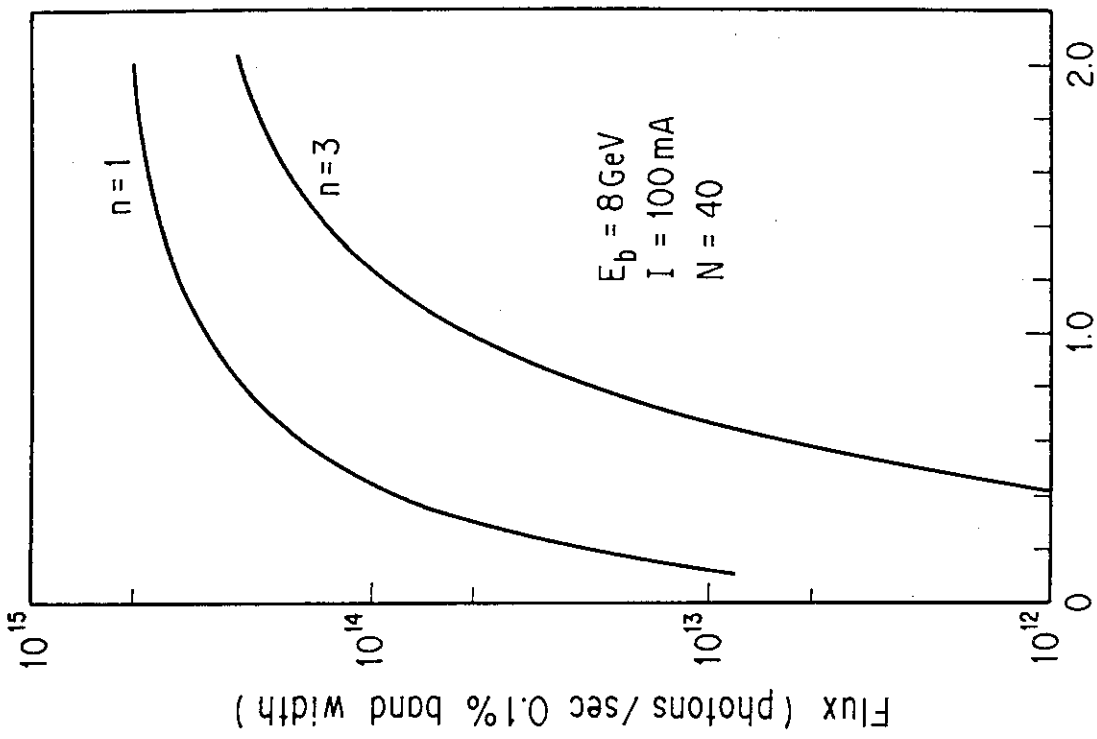

Fig.16 Flux of photon from an undulator as a function of K for the electron beam energy of 8 GeV, the beam current of 100 mA and the undulator period of 40.

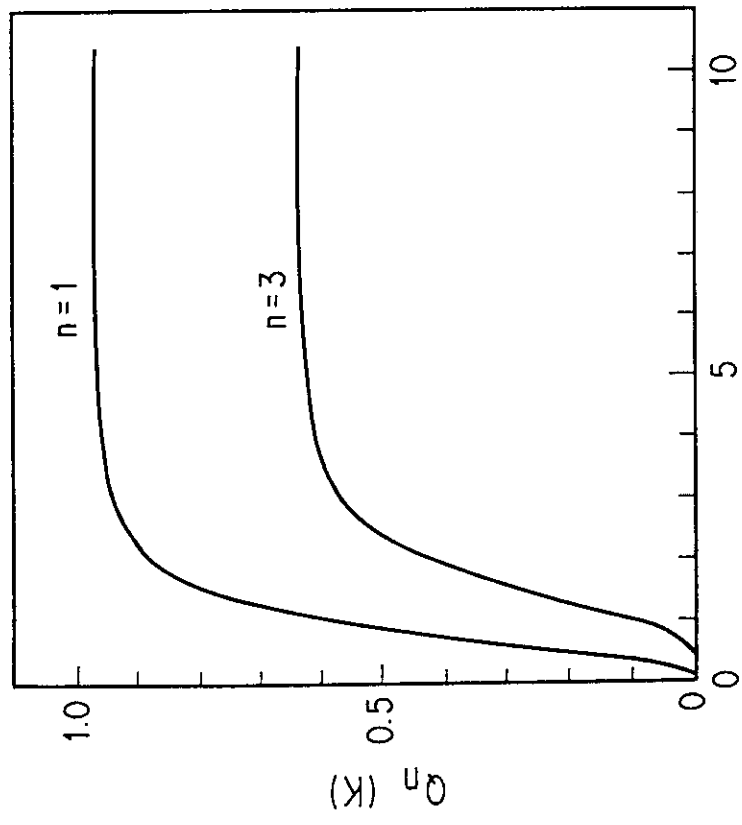

Fig.15 Plotting of the function $Q_n(K)$ as functions of harmonic number, n and deflection parameter, K.

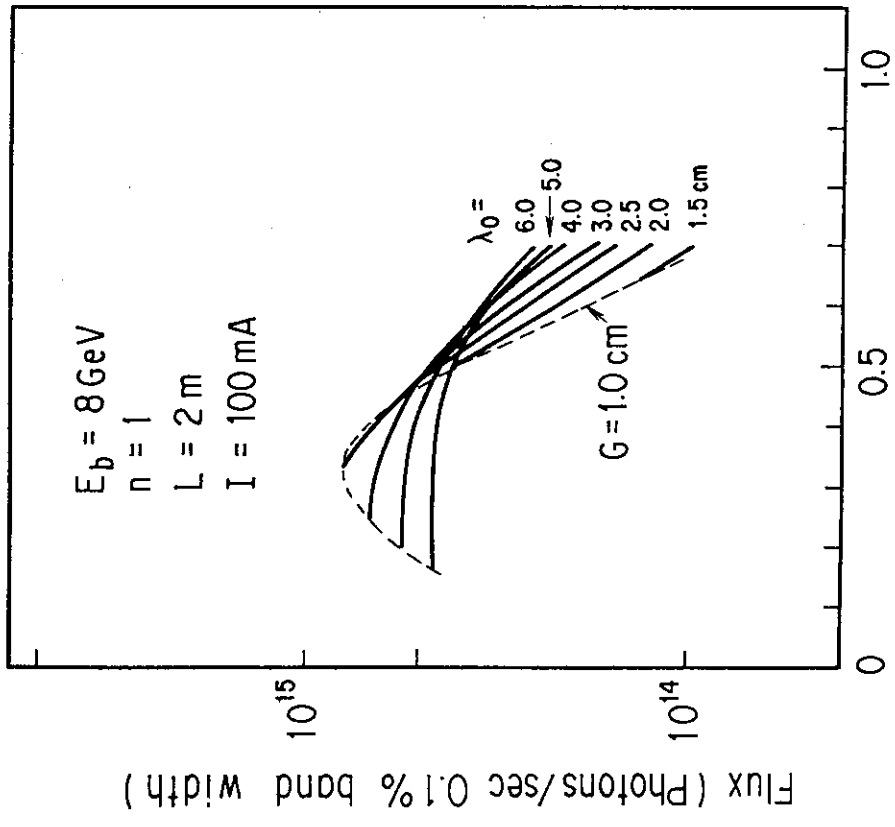

Fig.17 Flux of the fundamental harmonic photon as functions of the undulator period λ_0 and the ratio G/λ_0 of the undulator gap G to the period for the electron beam energy of 8 GeV, the undulator length of 2 m and the beam current of 100 mA.

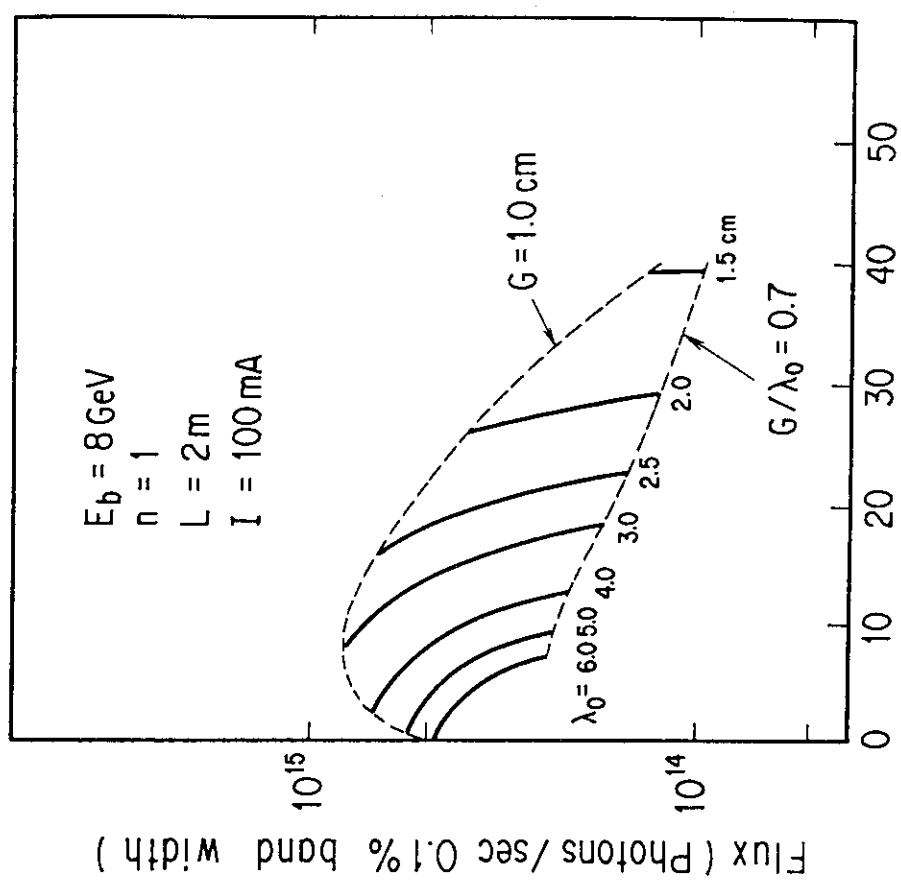

Fig.18 Flux of the fundamental harmonic photon as functions of the photon energy and the undulator period for the electron beam energy of 8 GeV, the undulator length of 2 m and the beam current of 100 mA.

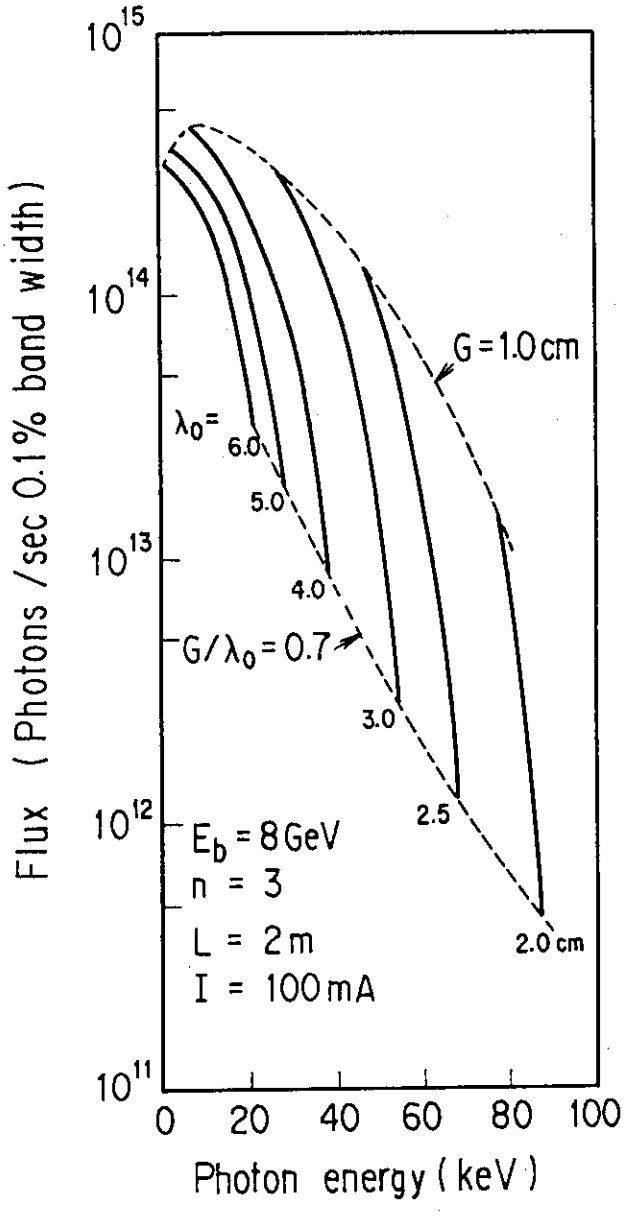

Fig.19 Flux of the third harmonic photon as functions of the photon energy and the undulator period for the electron beam energy of 8 GeV, the undulator length of 2 m and the beam current of 100 mA.

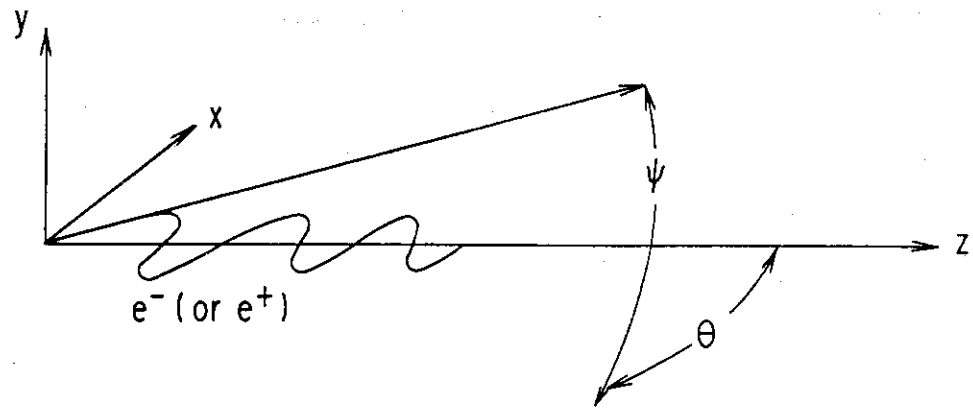

Fig.20 Electron trajectory and coordinate system in an undulator.

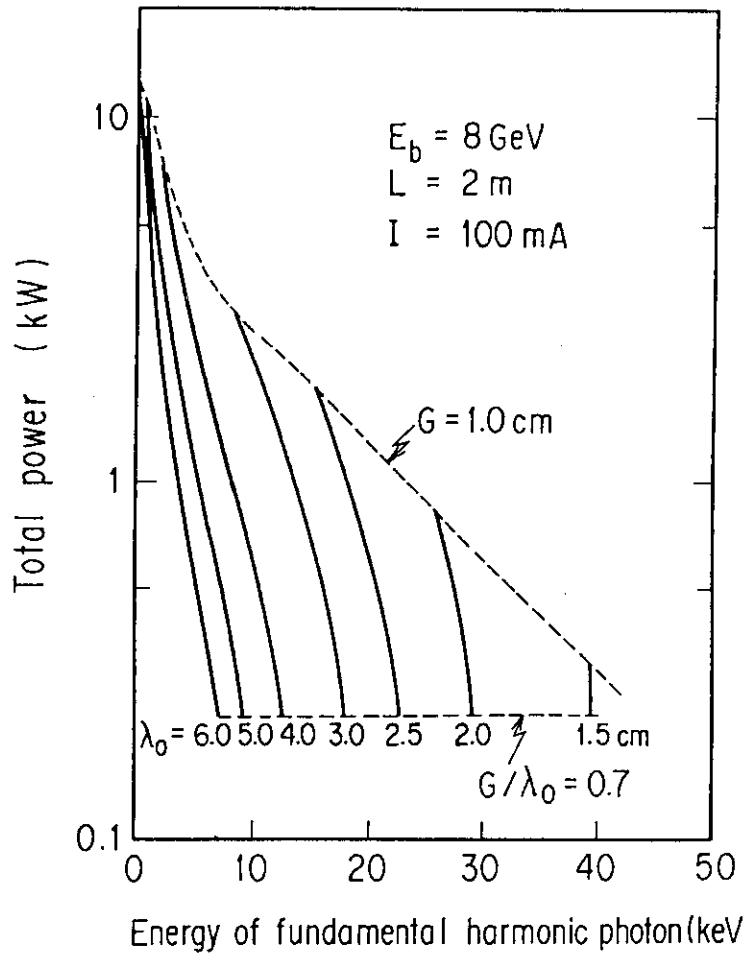

Fig.21 Total power of photon from an undulator as functions of energy of the fundamental harmonic photon and the undulator period for the electron beam energy of 8 GeV, the undulator length of 2 m and the beam current of 100 mA.

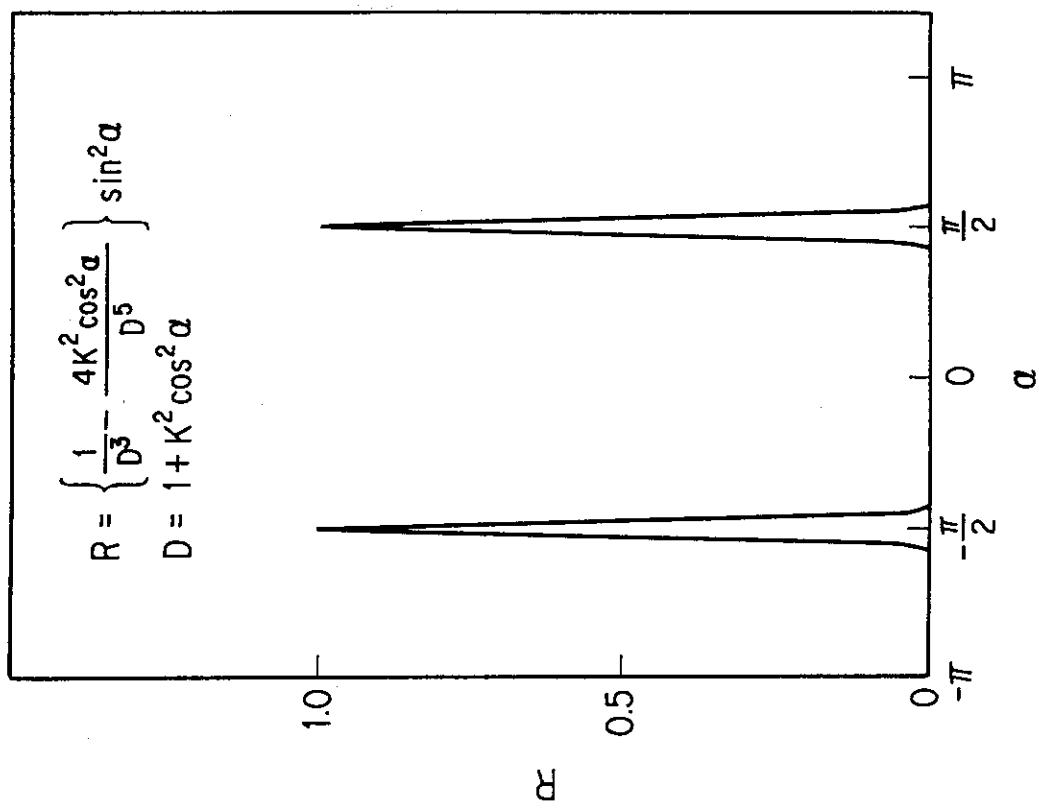

Fig.23 Plotting of the function U shown in eq. (32).

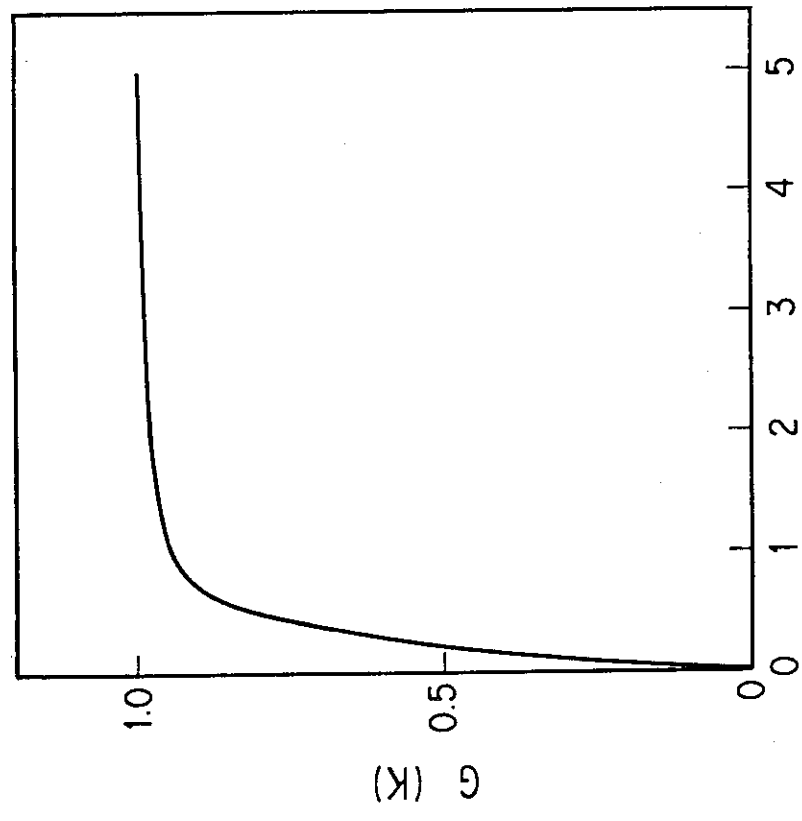

Fig.22 Plotting of the function G(K) as a function of deflection parameter K.

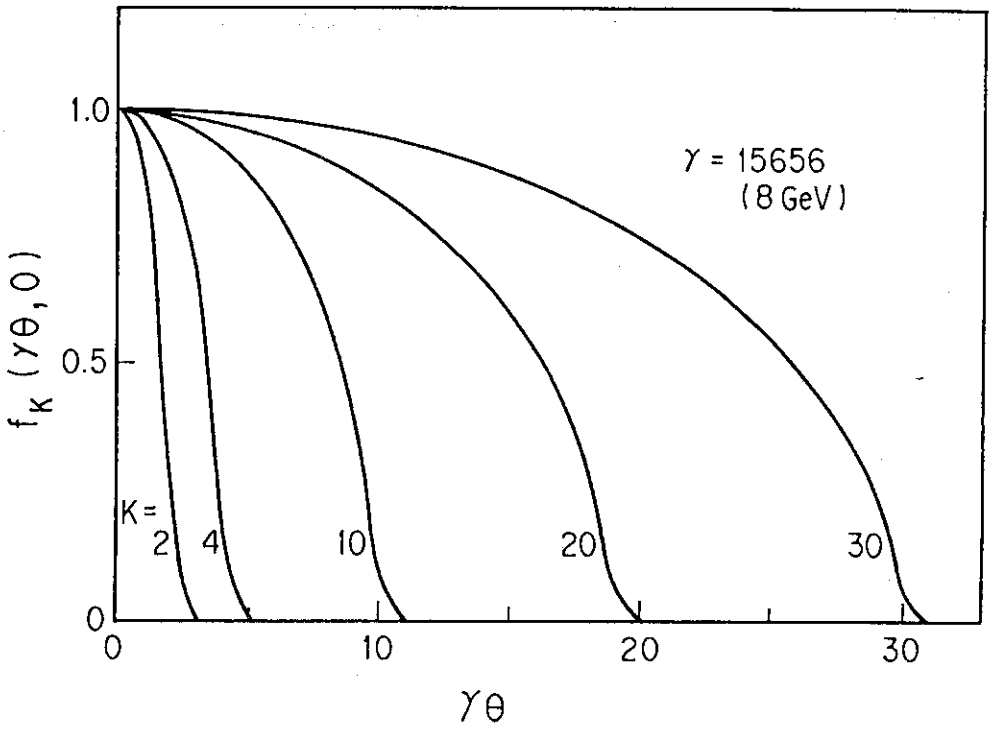

Fig.24 Plotting of the function $f_K(\gamma\theta,0)$ as functions of K and $\gamma\theta$.

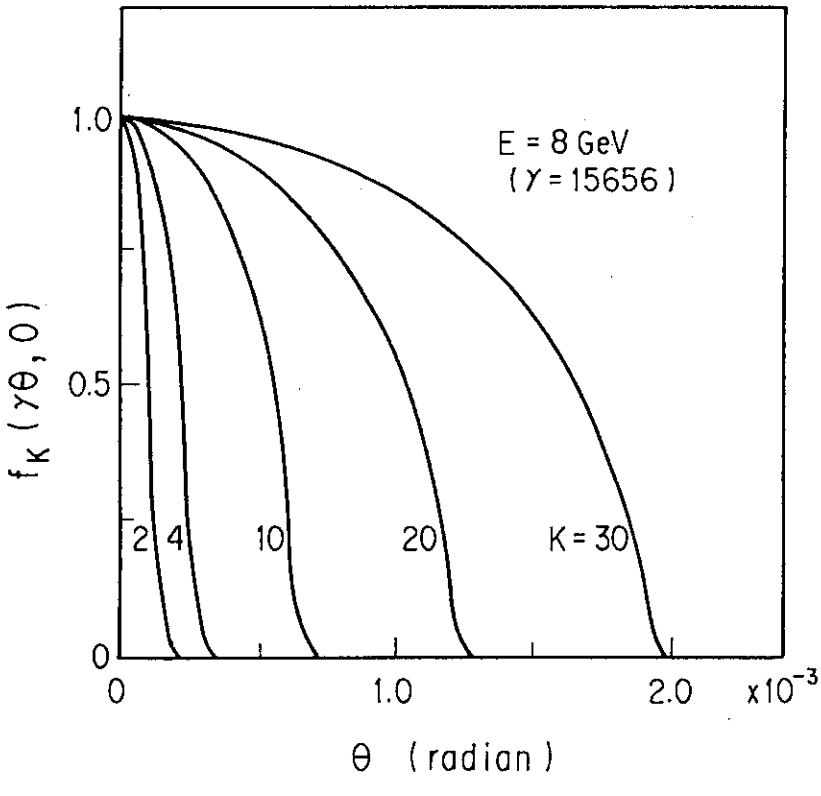

Fig.25 Plotting of the function $f_K(\gamma\theta,0)$ as functions of K and θ.

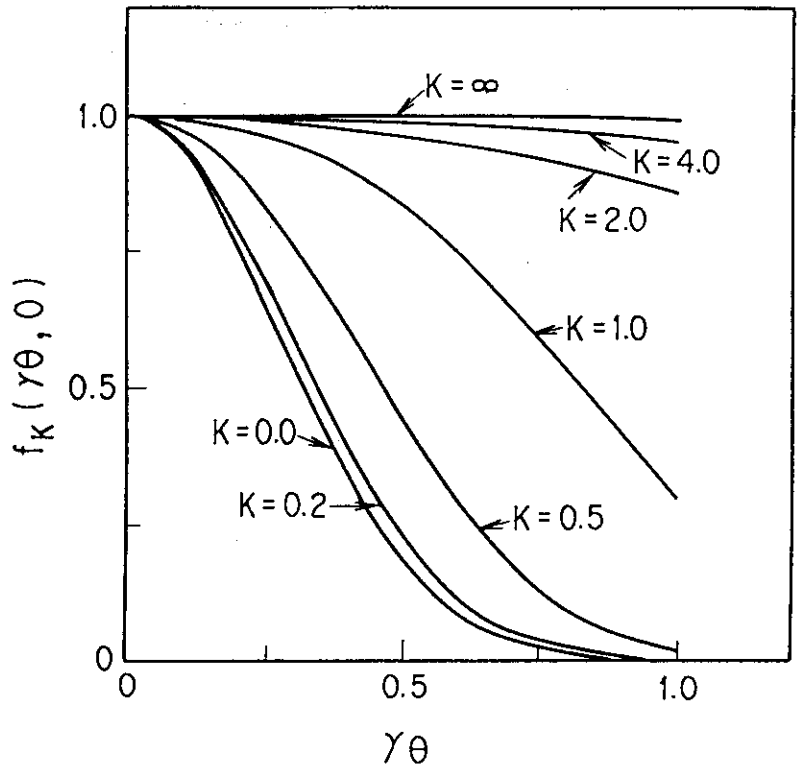

Fig.26 Plotting of the function $f_K(\gamma\theta.0)$ as functions of K and $\gamma\theta$.

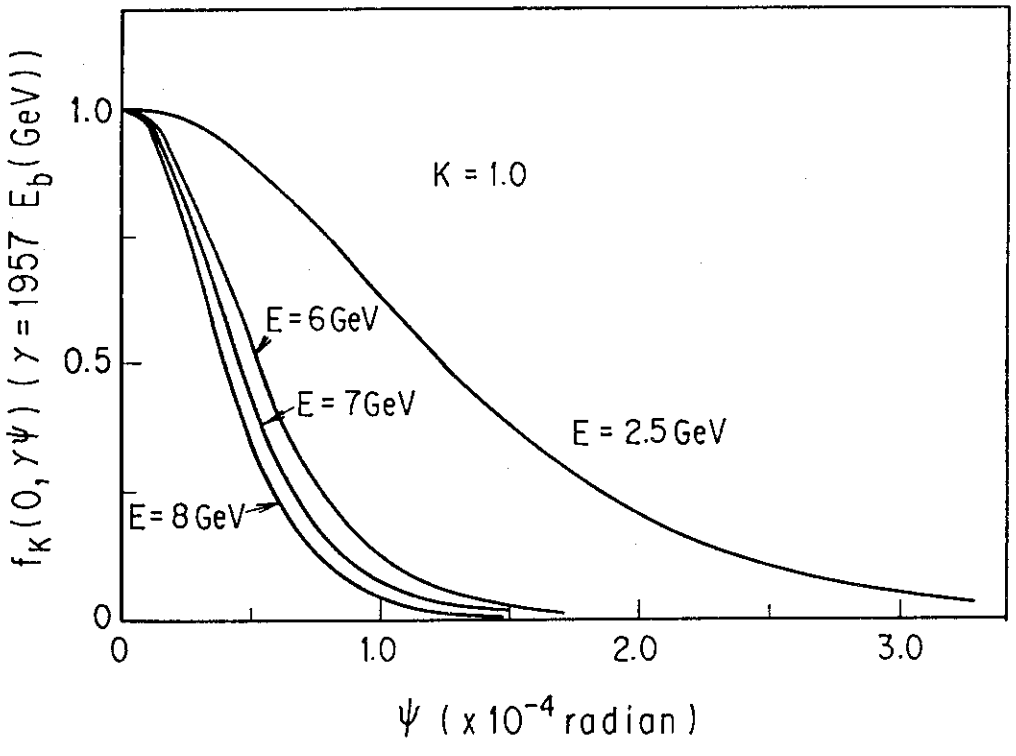

Fig.27 Plotting of the function $f_K(0, \gamma\psi)$ as functions of K ,ψ and the electron beam energy.

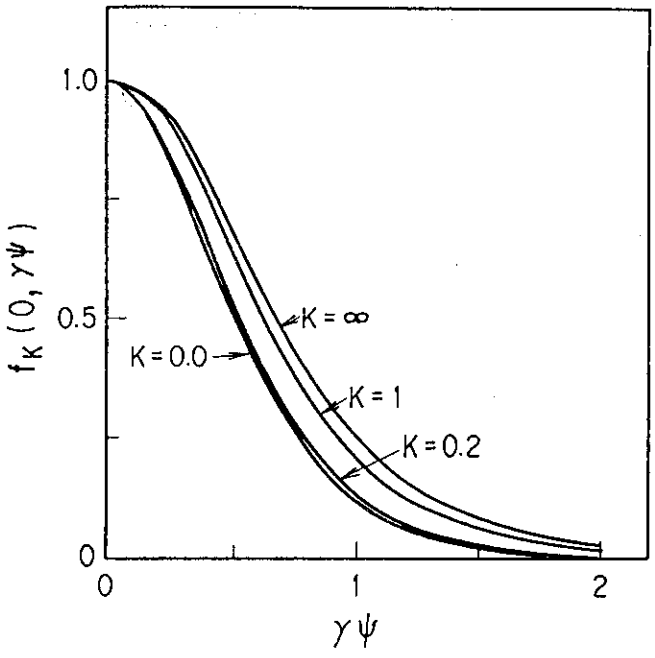

Fig.28 Plotting of the function $f_K(0,\gamma\psi)$ as functions of K and $\gamma\psi$.

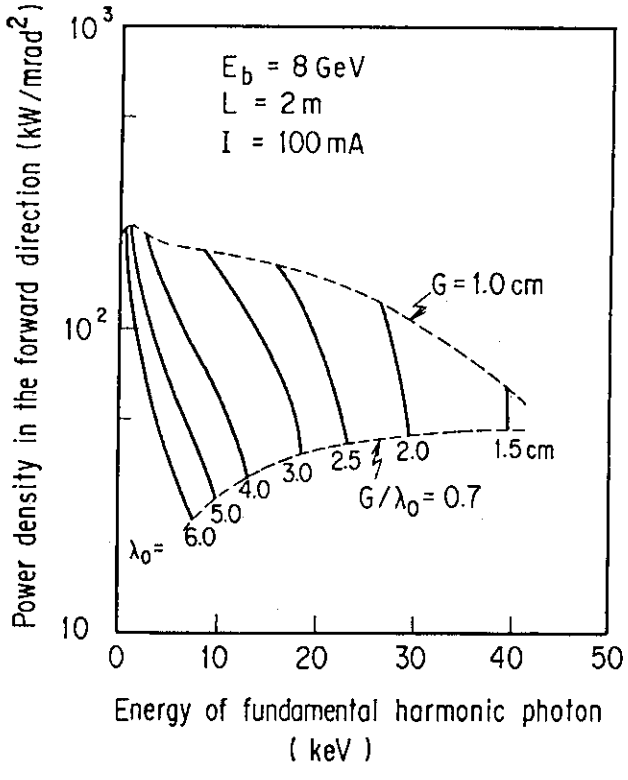

Fig.29 Power density of photon in the forward direction as functions of the fundamental harmonic photon energy and the undulator period for the electron beam energy of 8GeV , the undulator length of 2 m and the beam current of 100 mA.

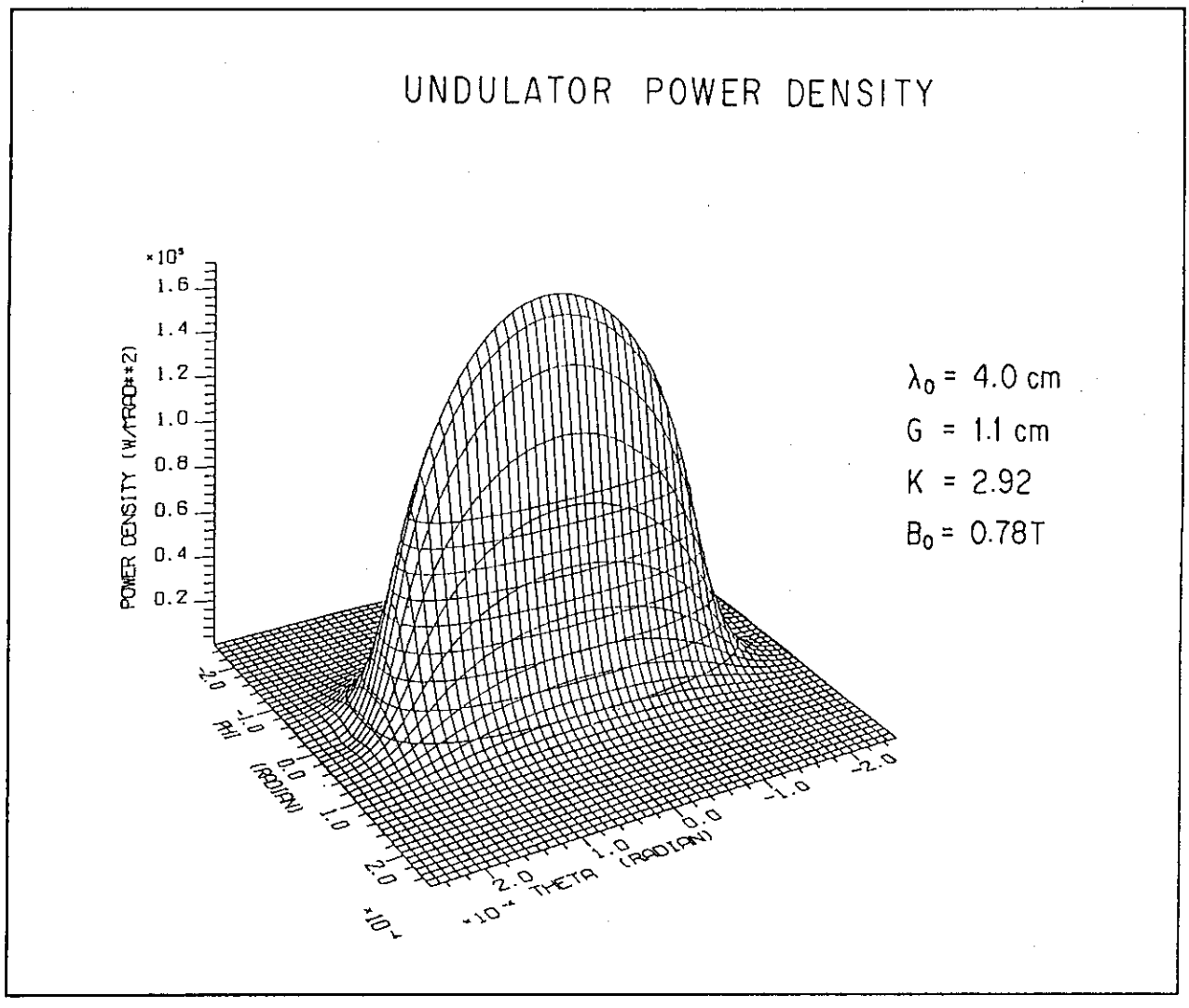

Fig.30 Angular power distribution of photon from an undulator with the value of K = 2.92.

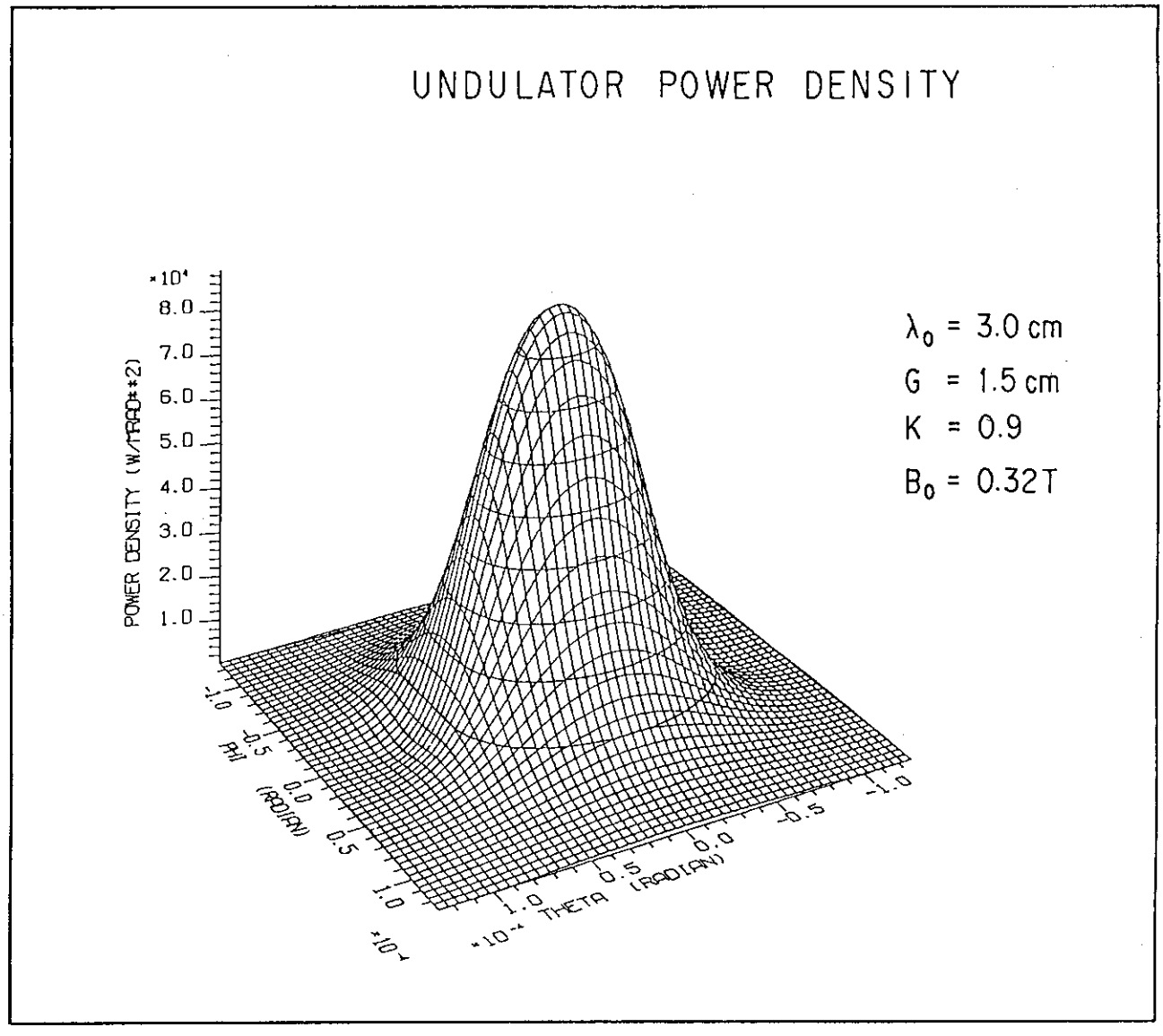

Fig.31 Angular power distribution of photon from an undulator with the value of K = 0.90.

5. CONCLUDING REMARKS

This paper described the flux and power spectra of the synchrotron photon from bending magnets and insertion devices in a 8 GeV storage ring(electron beam current of 100 mA). The power spectra plays an important role for heat generation on the optical devices in a beam line for a high brilliant synchrotron photon facility. The numerical studies show the following results.

(1) The bending magnet with the field strength of 0.6 tesla provides the critical energy of 25.5 keV and the maximum photon flux of 1.8×10^{13} photon/sec 0.1 % band width.
Each bending magnet with the bending angle of 65 milliradians produces the total power of 8.7kW. The power integrated over all vertical angles is 133 W/mrad, whereas the peak power density in the horizontal plane is 1.33 kW/mrad^2.
The storage ring having 96 dipoles radiates the total power of 835 kW.

(2) The energy shifter increases the critical energy to 127.7 keV at the magnetic field of 3 tesla.

(3) The multipole wiggler can yield the maximum photon flux of 1.5×10^{15} photons/sec o.1 % band width.
The total radiated power from a wiggler with the peak magnetic field of B_0= 1.0 tesla and the length of 4 m is 16.2 kW.
The peak power density is 178 kW/mrad^2 in the forward direction.

(4) The undulator with the length of 2 m can provide the flux of the fundamental and third harmonic photon to be in the order of 10^{14} photons/sec 0.1 % band width.
The undulator of the length of 2 m and the peak magnetic field of 0.4 tesla yields the total power of 1.3 kW.
The power density in the forward direction is expected to be between 100 ~ 200 kW/mrad^2, depending on the undulator period and gap.

The angular distribution of synchrotron photon from insertion devices is important because the width of the undulator spectra is broadened due to electron beam divergence. In the following the angular broadening of the peak will be studied.

REFERENCES

(1) E. E. Koch, ed., Handbook on Synchrotron Radiation (Elsevier, New York, 1983).

(2) T. Harami, "Undulator Sources at a 8 GeV Storage Ring", JAERI-M 89-066 (1989).

(3) G. K. Green, "Spectra and Optics of Synchrotron Radiation",BNL 50522 (1976).

(4) G. Brown, K. Halbach, J. Harris and H. Winick, "Wiggler and Undulator Magnets-A Review", Nucl. Instr. Meth. 208, 65-77 (1983).

(5) G. K. Shenoy and P. J. Viccaro, "An Overview of the Characteristics of the 6 GeV Synchrotron Radiation: A Preliminary Guide for Users", ANL Report ANL-85-69 (1985).

(6) D. F. Alferov, Yu. A. Bashmakov and E. G. Bessonov, "Undulator Radiation", Sov. Phys. Tech. Phys., 18, 1336-1339 (1974).

(7) K. J. Kim, "Angular Distribution of Undulator Power for an Arbitrary Deflection Parameter K", Nucl. Instr. Meth. A246, 67-70 (1986).

Appendix 1 Beam Emittance and Storage Ring Lattice

To achieve a small electron emittance, the double focusing achromat lattice, so-called the Chassman-Green lattice has been investigated. The ideal minimum beam emittance in this lattice type assuming small bending angles and an isomagnetic ring with the damping partition number $J_x = 1$ can be given by[1]

$$\varepsilon_{CG}(m \cdot rad) = 5.036 \times 10^{-13} E_b^2(GeV) \Theta^3(deg). \quad (A.1)$$

This equation shows the cubic dependence of the beam emittance on the deflection angle Θ of a bending magnet and the square dependence of the beam emittance on the electron (or positron) beam energy. This point leads to small deflection angles of the bending magnets, that is, the ring lattice with many unit cells, in order to achieve a small beam emittance. In figure A.1, the ideal minimum beam emittance and the cell number in a storage ring are shown as functions of the bending angle and the electron (or positron) beam energy. The storage ring can have a similar minimum beam emittance 2.2 ~ 2.3 nm·rad for the cell numbers 36, 40 and 44 in the ring energies 6, 7, and 8 GeV, respectively. For the cell number of 48 in a 8 GeV ring, the ideal beam emittance is obtained from (A.1) to be 1.7 nm·rad.

In the actual ESRF lattice, the beam emittance is expected to be larger by a factor of three than the ideal one calculated from eq (A.1).

REFERENCES

(1) H. Wiedemann, "Low Emittance Storage Ring Design", SSRL ACD-NOTE 50 (1986).

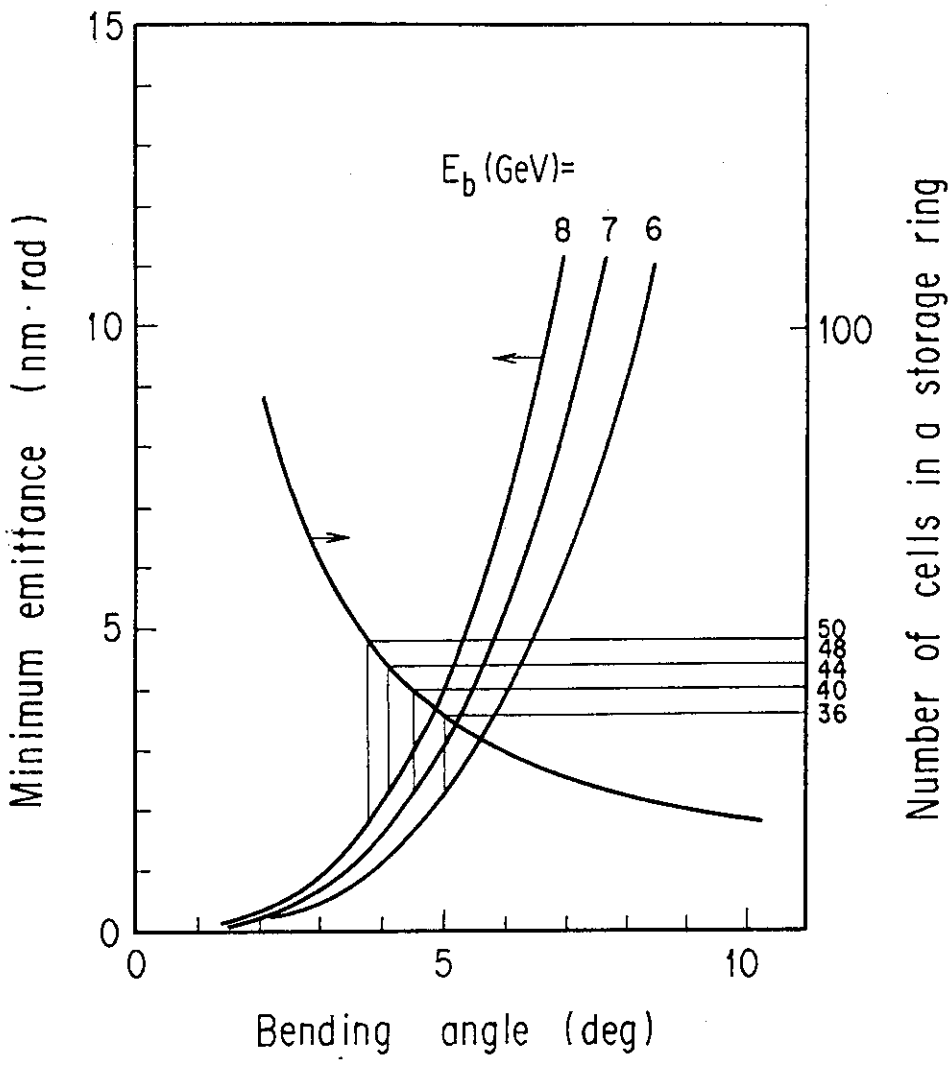

Fig.A.1 Minimum beam emittance and cell number in a storage ring as functions of bending angle and electron beam energy.

Appendix 2 Bending Magnet in a Storage Ring

If an electron is moving in a circular path in magnetic field B_{BM}, the radius of curvature of the electron trajectory is

$$\rho_{BM}(m) = \frac{3.335E_b(GeV)}{B_{BM}(T)}, \tag{A.2}$$

and the energy radiated per turn is[1]

$$U_0(\text{keV per electron turn}) = \frac{88.5E_b^4(GeV)}{\rho_{BM}(m)} = 2.65E_b^3(GeV)B_{BM}(T). \tag{A.3}$$

The length of a bending magnet, L, is related to the deflection angle, Θ, of a bending magnet and is given by

$$L(m) = \rho_{BM}(m) \cdot \frac{\pi}{180}\Theta. \tag{A.4}$$

Figures A.2 through A.4 show U_0, B_{BM} and L as functions of the bending radius, ρ, and the electron beam energy ,E_b. The power in kW radiated in an electron storage ring at energy E_b and current I(A) is

$$P(kW) = \frac{88.5I(A)E_b^4(GeV)}{\rho_{BM}(m)} = 2.65E_b^3(GeV)I(A)B_{BM}(T). \tag{A.5}$$

The ring current in amperes is related to the number of electrons and to the revolution frequency,

$$\frac{I(A)}{10} = n_e\frac{e}{c}f = \frac{n_e e}{2\pi\rho_{BM}}. \tag{A.6}$$

P is multiplied by $10^{-3}/2\pi$ to give the equation[1]

$$P(W/\text{mrad}\theta) = 14.09E_b^4(GeV)I(A)/\rho_{BM}(m). \tag{A.7}$$

P is multiplied by Θ to obtain the total power intercepted from arc Θ

$$P\times\Theta = 1.263E_b^2(GeV)B_{BM}^2(T)L(m)I(mA). \tag{A.8}$$

REFERENCES

(1) G. K. Green, "Spectra and Optics of Synchrotron Radiation", BNL 50522 (1976).

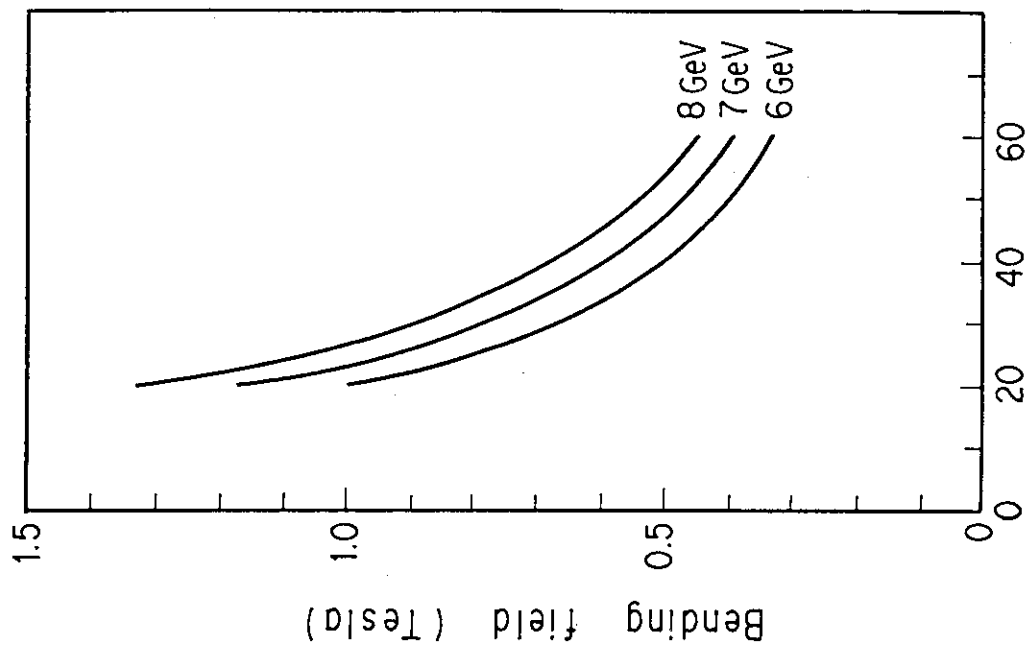

Fig.A.3 Bending field as functions of the bending radius and the electron beam energy.

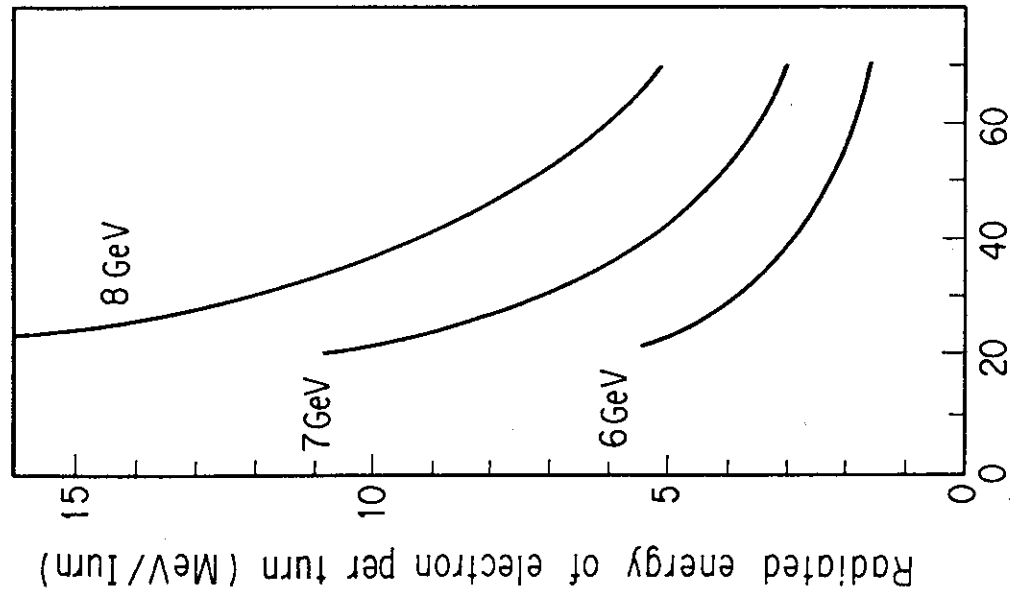

Fig.A.2 Radiated energy of electron per turn as functions of the bending radius and the electron beam energy.

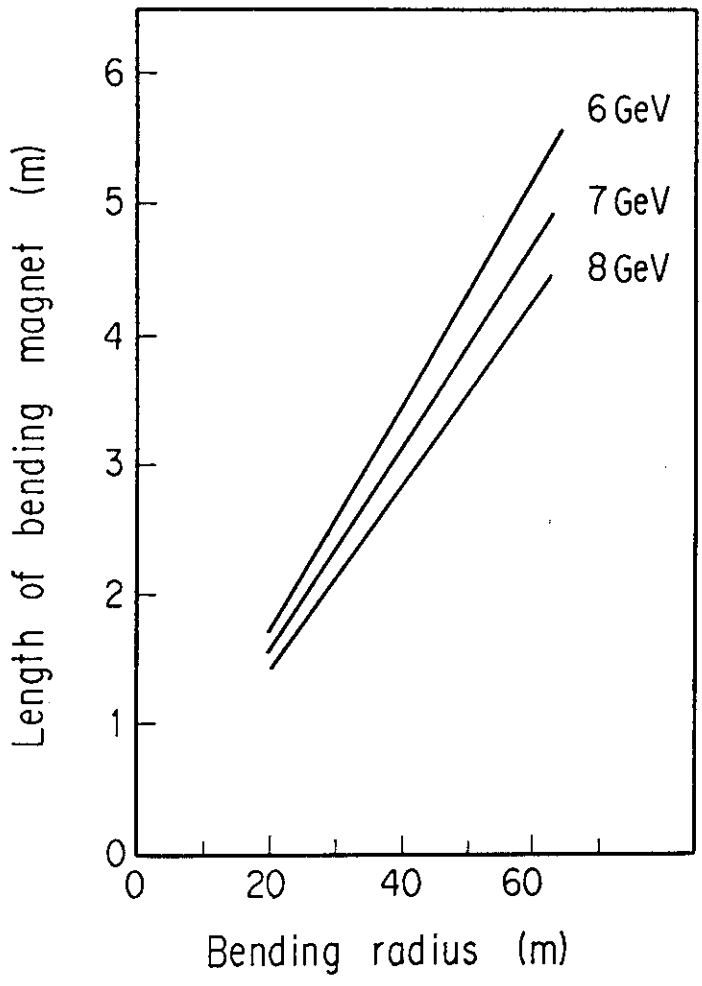

Fig.A.4 Length of bending magnet as functions of the bending radius and the electron beam energy.